FUSELAGE AND NACELLE EFFECTS ON AIRPLANES AS DETERMINED BY A STATISTICAL STUDY OF DATA FROM THE GALCIT 10-FOOT WIND TUNNEL

Thesis

by

Edgar P. Williams

In Partial Fulfillment of the

Requirements for the Degree of Aeronautical Engineer

California Institute of Technology

Pasadena, California

1942

TABLE OF CONTENTS

ACKNOWLEDGEMENT

The author wishes to express his appreciation for the suggestions given him by Drs. C. B. Millikan, H. J. Stewart, A. L. Klein and Mr. R. E. Marquardt.

INDEX OF FIGURES

Table I

NOTATION

C_{D_s} ≡ Fuselage drag coefficient based on wetted area of fuselage

$C_{D_{fr}}$ ≡ Drag coefficient based on maximum frontal or proper area

F. R. = Fineness Ratio ≡ $\frac{\text{length of body}}{\text{average diameter of body}}$

Average diameter = $2\sqrt{\frac{S_{fr}}{\pi}}$

$C_{m_{F_1}} \equiv \frac{M}{q\, S_{fr}\, L}$

(Where S_{fr} is the frontal area of fuselage)

L = Fuselage length

$C_{m_{F_2}} \equiv \frac{M}{q\, w\, L^2}$

w = maximum fuselage width

$x_{c.g.}$ = distance from fuselage nose to center of gravity

$C_m = \frac{M}{qS_w\,(m.s.c.)}$

C_{m_o} = C_m at $C_L = 0$

i_w ≡ Angle between zero lift lines of fuselage and wing

c ≡ Root chord

SUMMARY

An attempt to base fuselage drag upon wetted area showed no less scatter than C_{D_π} as a function of fineness ratio. For average values of C_{D_π} for fuselages and flying boat hulls see Figure 12.

The destabilizing effect of fuselages and flying boat hulls based on the volume of a circumscribed cylinder is given in figure 22 as a function of the c.g. position. The fuselage body appears to act somewhat analogous to an airfoil with an aerodynamic center at a point somewhere between the 0.2 and 0.3 body position.

The effect of fuselages and flying boat hulls on C_{m_o} is given by figures 23 through 29. One set of figures gives C_{m_o} as a function of the destabilizing effect and the other set as a function of the c.g. position.

No successful means of correlating nacelle data was found. Figures 30 through 33 show the magnitude of nacelle drag and moment effects.

1. INTRODUCTION

All data used in this report were obtained from tests conducted in the closed working section of the 10-foot wind tunnel of the GALCIT (Guggenheim Aeronautics Laboratory, California Institute of Technology). (Figure 1) The critical Reynolds Number at which a 15 cm. sphere has a drag coefficient of 0.3 is about 325,000 which indicates that the tunnel wind stream has a fairly low turbulence. (cf. reference 1) Practically all data used here were obtained at a dynamic pressure of $q = 35$ gm/cm^2, corresponding to a tunnel air speed of about 176 m.p.h. for air of a density ratio $\rho/\rho_0 = 0.91$. The Reynolds Number for these tests (based on the mean wing chord of an average sized model) was of the order of 1×10^6. With one exception all data were obtained using the wire suspension system which was in use prior to October, 1942. * (Figure 2) The exception consisted of a fuselage of unusually high fineness ratio which was desired to augment the range of fuselage data.

All models considered were tested during a period of years extending from 1930 through 1941, and in most cases the tests were conducted by the GALCIT staff for various aircraft companies. Unless otherwise stated, all data were derived from conventional, modern, cantilever monoplanes many of which are in service today.

Fuselage and nacelle effects were obtained by taking the difference of two runs, e.g., wing plus fuselage minus wing alone. Thus all data include interference effects. The one exception to this is the drag of the Goodyear-Zeppelin Airship, Akron, which is included for reference in the fuselage drag curves.

* A triple strut suspension system permitting six component force measurements at angles of yaw is now in use at the GALCIT.

11. FUSELAGE EFFECTS

A. Drag

The author had hoped to reduce the scatter generally found in the proper drag coefficient, $C_{D_{fp}}$, for a fuselage by basing drag on the total surface area of the fuselage, obtaining essentially a skin friction drag coefficient, C_{D_s}. (Reference 2)

Multi-engine land airplanes were chosen as the most favorable class for such an investigation as the fuselages of this type approach more closely a perfectly streamlined form than either flying boat hulls or single engine fuselages for which the cockpit enclosure is relatively large. Considerable time was spent in determining surface areas of a number of fuselages of this class from drawings in the GALCIT files. For each fuselage a curve of $p/\cos\theta$ vs. fuselage station was plotted. Where:

p = fuselage perimeter at any station

θ = acute angle between a tangent to the fuselage at the corresponding station and the fuselage reference line

Now:

$$S_s = \int_0^L \frac{p}{\cos\theta}\, dL$$

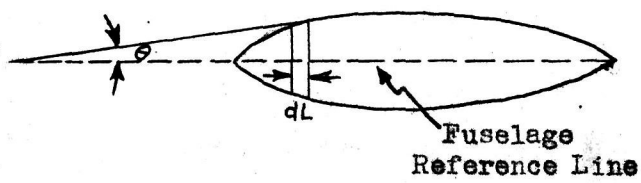

Where:

S_s = total fuselage surface area or wetted area of fuselage

L = fuselage length

dL = element of axial length

Thus the total fuselage surface area, S_s, is given by the area under the curve which was obtained with a planimeter. This

method is rigorous but laborious. The results are tabulated in Table 2 and plotted against Reynolds Number (based on fuselage length) in Fig. 3. The results show a scatter (defined as $\frac{\text{maximum variation from average}}{\text{average}}$) of about 26%.

Figure 4 gives the same data broken into two groups according to fuselage cross-section and fig. 5 is identical with fig. 4 except that all fuselages with cockpit enclosures have been omitted. The scatter is still great even for the most favorable group, circular fuselages with no cockpit enclosures (fig.5).

One reason for this scatter is indicated in fig. 3 by the variation in drag of the dirigible model with Reynolds Number. Comparing this with Karman's turbulent skin friction curve (reference 3), it is evident that the average fuselage model in the GALCIT 10-foot tunnel lies within the transition region from laminar to turbulent flow somewhere near the turbulent side of the region.

Another important factor is wing-fuselage interference. An interesting example is given by GALCIT Reports 291 and 298 in which the same fuselage was tested with two different wings, identical in planform, and differing only in airfoil section. One wind was smooth whereas the other had flap brackets. When tested with the smooth wing, the fuselage drag increment was 25 drag points ($C_{D_p} = 0.0025$ based on wing area) more than its drag increment when tested with the wing equipped with flap brackets. The flap brackets, however, increased the wing drag 34 points, leaving a net overall drag increase due to flap brackets in the presence of the fuselage of only 9 drag points.

This example deterred the author from attempting to correlate interference drag with the vertical position of the wing as he had hoped to do.

C_{D_π} (based on maximum projected frontal area) is plotted versus fineness ratio in fig. 6 for the same fuselages considered in fig. 3. Here the scatter is less than 24%, or slightly less than for C_{D_s}. Therefore despite the more fundamental nature of the coefficient C_{D_s}, it was decided that the time involved in computing wetted areas was not warranted and all remaining fuselage drags were based only on proper areas.

All additional multi-engine, land airplane fuselage drags available were compiled. Fig. 7 includes the complete set of data for this class, and figure 8 gives a breakdown for the complete data according to two types of fuselage cross-sections, with and without cockpits. Fig. 8 corresponds to figs. 4 and 5 except that fig. 8 includes some additional data. These three figures indicate that the drag coefficients of circular fuselages are generally slightly lower than for the square-round type, but that it is possible to obtain equally low drag coefficients with the latter type. Fuselages with cockpits generally have a higher drag as expected.

It should be noted that the slopes of the average drag value curves used in both figures 8 and 10 were chosen to coincide with that given in fig. 9. This slope is the rate of change of (wetted area/frontal area) with fineness ratio for smooth stream-lined forms. (Reference 4) However, this slope did not fit the drag data for flying boat hulls (fig. 11), so an average value was faired in by eye.

This curve should not be extrapolated far in either direction, for figure 12 indicates that it would cross the average drag curves for land airplanes at low fineness ratios.

B. Destabilizing Effect

Several attempts were made to correlate the destabilizing effect of fuselages with various parameters. For these preliminary attempts, only the most favorable class, multi-engine, land airplanes, was used.

The change in the slope of the pitching moment curve, $\Delta\left(\frac{dC_m}{dC_L}\right)$, due to the fuselage is plotted against the number of root chord lengths the fuselage extends ahead of the quarter root chord, $\frac{l}{c}$, in figure 13. The correlation is fairly good, but the author was not satisfied with the parameters involved. Actual fuselage effects should predominate over interference effects so more complete dimensions of the fuselage should be involved and the aft portion should have some effect. Perfect fluid theory (reference 5) gives the moment produced by a body of revolution as a function of its apparent mass, angle of attack, and of course the dynamic pressure. The apparent mass is a function of the volume and shape of the body.

Two parameter were tried, $C_{m_{F_1}}$ and $C_{m_{F_2}}$. They are defined as follows:

$$C_{m_{F_1}} = \frac{M}{qS_W L}$$

$$C_{m_{F_2}} = \frac{M}{qwl^2}$$

Where:

M = pitching moment due to fuselage (positive when stalling)

q = dynamic pressure, $\frac{1}{2}\rho V^2$

S = maximum projected frontal area of fuselage or proper area

L = fuselage length

w = maximum width of fuselage cross-section

Note that $C_{m_{F_1}}$ is based on the volume of a circumscribed cylinder. The volume of a fuselage is given by a constant times the volume of the circumscribed cylinder. For most fuselage shapes, this constant lies between 0.6 and 0.7 (ref. 6)

Perfect fluid theory gives a pure couple, but it was believed that the position of the axis about which moments are measured should be important. (To the author's knowledge, the moment acting on a figure of revolution in a viscous fluid has never been treated theoretically.) Figures 14 and 15 show the destabilizing effect of fuselages for multi-engine, land airplanes based on the two parameters defined above as a function of the center of gravity postion. (All moment data used in this report are given about an assumed center of gravity position.)

There appears to be no clear choice as far as scatter is concerned between these three methods. The method of figure 15 was chosen for further work only because fuselage volume is roughly proportional to the circumscribed cylinder and the volume is a more basic parameter.

Figures 16 and 17 were drawn up to determine the effect of fuselage cross-section and vertical c.g. position. No consistent variation with either is shown by these curves. However it is believed that the variation in the vertical c.g. position is responsible for much of the scatter. It should be mentioned that in finding $\Delta\left(\frac{dC_m}{dC_L}\right)$, the moment curves were approximated by straight lines over a C_L range of from 0.0 to about 0.6. In many cases there was sufficient curvature in the moment curves to make this method unsatisfactory.

Figure 18 is identical with figure 15 except that additional data have been added. The two low points falling just outside the indicated band of scatter are of interest. As the sketch indicates, the aft portion of the two fuselages was abnormally small. In one case the aft portion was partially faired in with wax and the destabilizing effect was increased slightly, placing the fuselage just inside the lower band of scatter. No satisfactory explanation could be found for the unusually high destabilizing effect of the fuselage lying above the band of scatter. It consisted of a circular fuselage surmounted by a cockpit enclosure. The frontal area of the fuselage was unusually small relative to the wing thickness. Unfortunately no large drawing was available so the c. g. position was measured from a small three view, and there remains the possibility that the c.g. position indicated on the drawing was in error.

Figure 19 gives the destabilizing effect of fuselages of single engine airplanes. More scatter is to be expected because of the greater variation in fuselages of this type. Furthermore, the effect of air flow through the cowling doubtless accounts for considerable scatter.

The destabilizing effect of flying boat hulls is shown in figure 20. Figure 22 shows that this effect for hulls based on $C_{m_{F_1}}$ is lower than for fuselages of land airplanes. This is in line with the lower destabilizing effect of the two multi-engine land airplanes with small aft portions previously noted.

Note the extrapolated curves indicate that there should be no destabilizing effect were the c.g. at a point somewhere

between the 0.2 and 0.3 body position.

Because the aft portion was believed to have smaller effect for hulls, than for fuselages, figure 31 was plotted giving the variation of $\Delta\left(\frac{dC_m}{dC_L}\right)$ with the length of hull forward of the leading edge of the root chord in lengths of root chord.

C. Effect on Pitching Moment at Zero Lift, ΔC_{m_o}

Assuming the moment curves to be straight lines, we can find the change in moment at zero lift due to a fuselage as a function of the angle between the zero lift lines of the fuselage and the wing and the destabilizing increment, $\Delta\left(\frac{dC_m}{d\alpha}\right)$ due to the fuselage.

$$C_{m_o} = C_{L_1} \tan\delta$$

Where

$$\delta = \left\{ \frac{dC_m}{d\,C_L} \right\} \text{ due to fuselage}$$

$$C_{L_1} = 2\pi \eta_* i_w$$

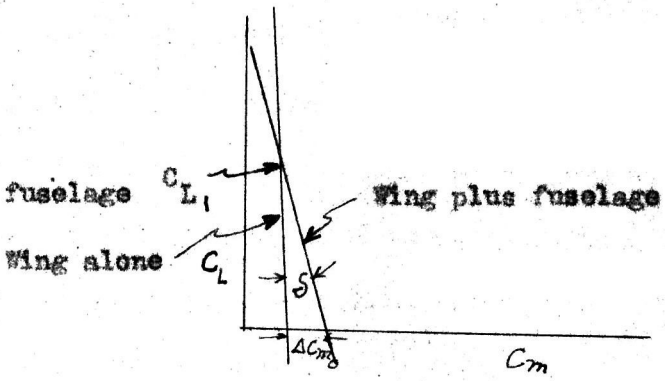

Where:

C_{L_1} is the lift coefficient at which the curves of wing alone and wing plus fuselage intersect.

η_* is the slope of the lift curve for the particular wing and aspect ratio concerned as measured from the wing alone curve. $\sim \frac{a_o}{1 + \frac{a_o}{\pi R}}$

i_w is the angle between the zero lift lines of the wing and the fuselage.

Since the zero lift line of the fuselage was not measured, it was assumed to be identical with the fuselage reference line. This should be satisfactory for a circular fuselage of a multi-engine land airplane with no cockpit, but it is undoubtedly a source of considerable error for single engine airplanes and flying boat hulls.

We have finally:

$$\Delta C_{m_o} = \frac{2\pi \eta_w}{57.3} \cdot i_w \Delta\left(\frac{dC_m}{dC_L}\right)$$

Or:

$$\Delta C_{m_o} = \Delta\left(\frac{dC_M}{d\alpha_w}\right) \times i_w^\circ$$

Figures 23, 24, and 25 show the results for the three classes of airplanes. Note that the average ΔC_{m_o} is somewhat greater than that indicated above. This is particularly noticeable in the case of flying boat hulls. This indicates that the zero lift line of an average fuselage or hull is tilted downward at the nose from the reference line. In view of the high aft portion of hulls and most fuselages, this is to be expected.

In reference 3 ΔC_{m_o} is plotted against i_w. Here the zero lift lines of the fuselages were faired in by eye. The report states that the data were corrected for the variation of c.g., but does not state specifically how this was done. ΔC_{m_o} was plotted as a function of i_w for the GALCIT data with no correction for the variation of c.g. position. There appeared to be no correlation whatsoever even for the most favorable case of multi-engine fuselages with no cockpits.

In order to obtain the effect of a fuselage on C_{m_o} independent of the destabilizing effect, $\frac{C_{m_{y_1}}}{i_w}$ versus $x\ \frac{c.g.}{L}$ was plotted. (Figures 26, 27, 28, and 29). Note that the square-round type fuselage has a greater effect than a circular fuselage. (Reference 8) This variation of effect with fuselage cross-section likely accounts for some of the scatter of the single engine fuselage data.

III. NACELLE EFFECTS

All nacelle data have been grouped into five classes according to vertical location with respect to wing chord at nacelle and number of engines. Data from nacelles with cooling flow have been segregated.

A. Drag

Nacelle drag coefficients based upon frontal area, $C_{D_{\pi}}$, are given in figures 30 and 31. As should be expected, the drag coefficient increases as the nacelles are lowered since a smaller percentage of the nacelle area is blanketed by the wing for the lower nacelles.

B. Destabilizing Effect

Two attempts were made to reduce the destabilizing effect of nacelles to a function of the distance the nacelle extends ahead of the leading edge of the wing in length of wing chord at the nacelle. In one case the moment coefficient was based on the frontal area of the nacelle times the wing chord at the nacelle center-line, $C_{m_{F_1}}$ and in the other on the maximum width of the nacelle times the square of the wing chord at the nacelle, $C_{m_{F_2}}$. The latter method was suggested by reference 9. Neither method gave satisfactory correlation so the plotted results are not included, but the data are recorded with the tabulated data.

The magnitude of the destabilizing effect of nacelles is shown in figure 32.

C. Effect on Pitching Moment at Zero Lift, ΔC_{m_o}

Since no satisfactory parameters were found for the destabilizing effect, no attempt was made to do so for ΔC_{m_o}. Figure 33 serves to indicate the magnitude of ΔC_{m_o}.

Suggestions for Future Work

If more accurate statistical moment data is desired it would likely be necessary to account for the vertical c.g. position and curvature of the moment curves.

Dr. H. J. Stewart has suggested considering the actual slope of the lift curve of the wing in empennage efficiency calculations rather than assuming a constant slope of $a_o = 5.7$ or 5.5 as is done at present in GALCIT calculations.

REFERENCES

1. Millikan, C. B., and Klein, A. L.: Description and Calibration of 10-foot Wind Tunnel at California Institute of Technology. Sixth Int. Aero. Meeting, A.S.M.E., 1932

2. North, V. T.: A Method for Predicting the Parasite Drag of Airplanes. A.C.T.R. 4608 (Restricted)

3. von Karman, Th.: Turbulence and Skin Friction. Jour. Aero. Sci., Vol. 1, January, 1934.

4. Lee, J. G.: Air-Cooled vs Liquid-Cooled Aircraft. Jour. Aero. Sci., Vol. 8, April, 1941.

5. Lamb, H.: Hydrodynamics. Cambridge University Press

6. Liepmann, H.P.: An Improved Longitudinal Stability Calculation. Jour. Aero. Sci., Vol. 9, March, 1942.

7. Hutchinson, J. L., and Priestley, E.: Note on the Effect of the Body on the Pitching Moment of a Wing. R. A. 1530 (Confidential)

8. Stephens, A. V.: Das Trudeln von Flugzeugen (The Spinning of Airplanes) Luftfahrtforschung, Vol. 11, October, 1934.

9. Smith, F., and Smelt, R.: Note on Pitching Moment Changes due to a Nacelle on a Wing. R. A. 1494 (Confidential)

10. Seiferth, R.: Wind Tunnel Tests on a 1/75 Scale Model of the Goodyear-Zeppelin Airship 'Akron' Z. R. 3. 4 with Normal and Ring Tail Surfaces. Pacific Coast Aero. Meeting, A.S.M.E., 1932.

11. Jacobs, E. N., and Ward, K. E.: Interference of Wing and Fuselage From Tests of 209 Combinations in the N. A. C. A. Variable-Density Tunnel. N.A.C.A. T. R. 540

VERTICAL SECTION THROUGH 10 FT. WIND TUNNEL

GUGGENHEIM AERONAUTICS LABORATORY
CALIFORNIA INSTITUTE OF TECHNOLOGY, PASADENA

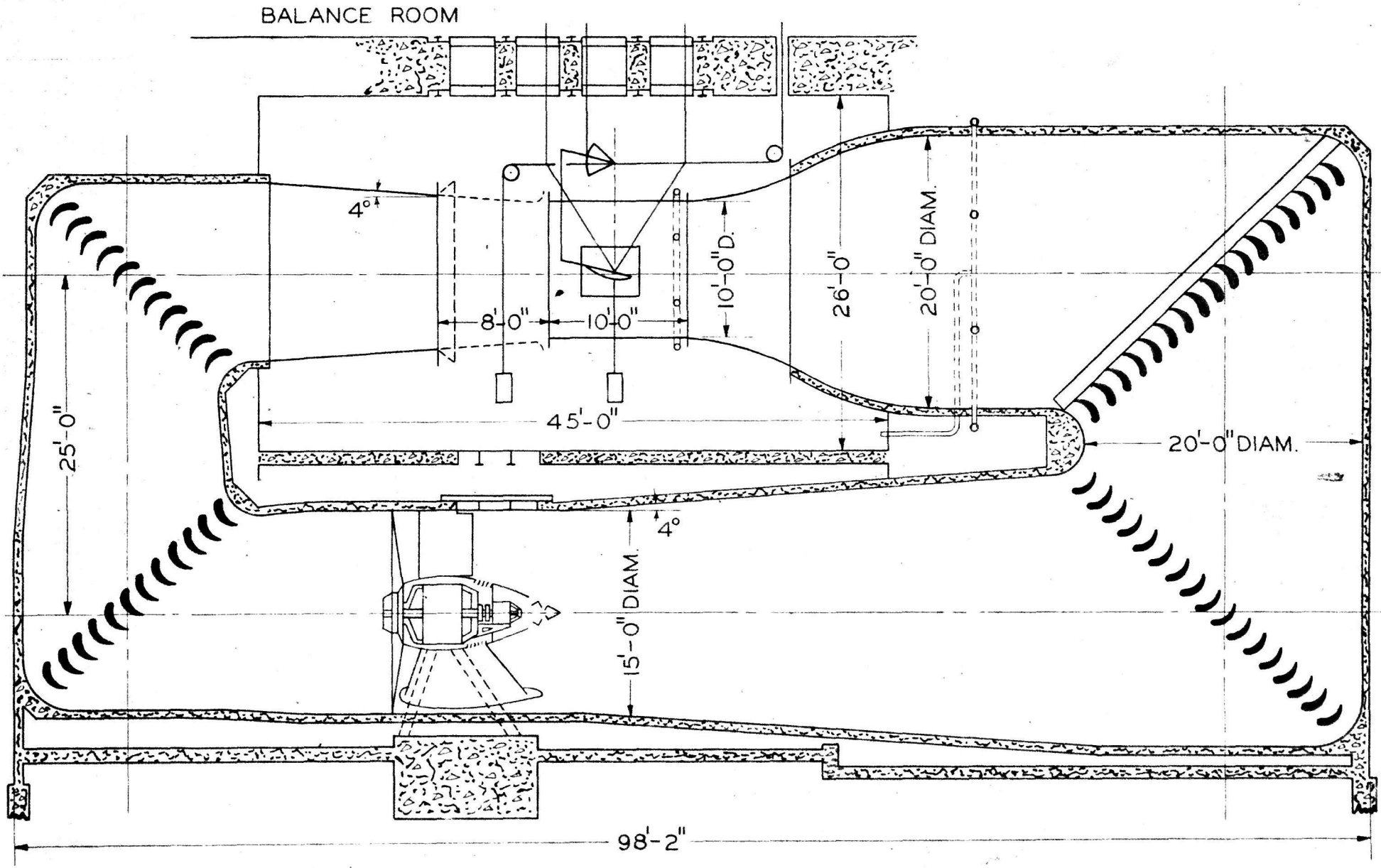

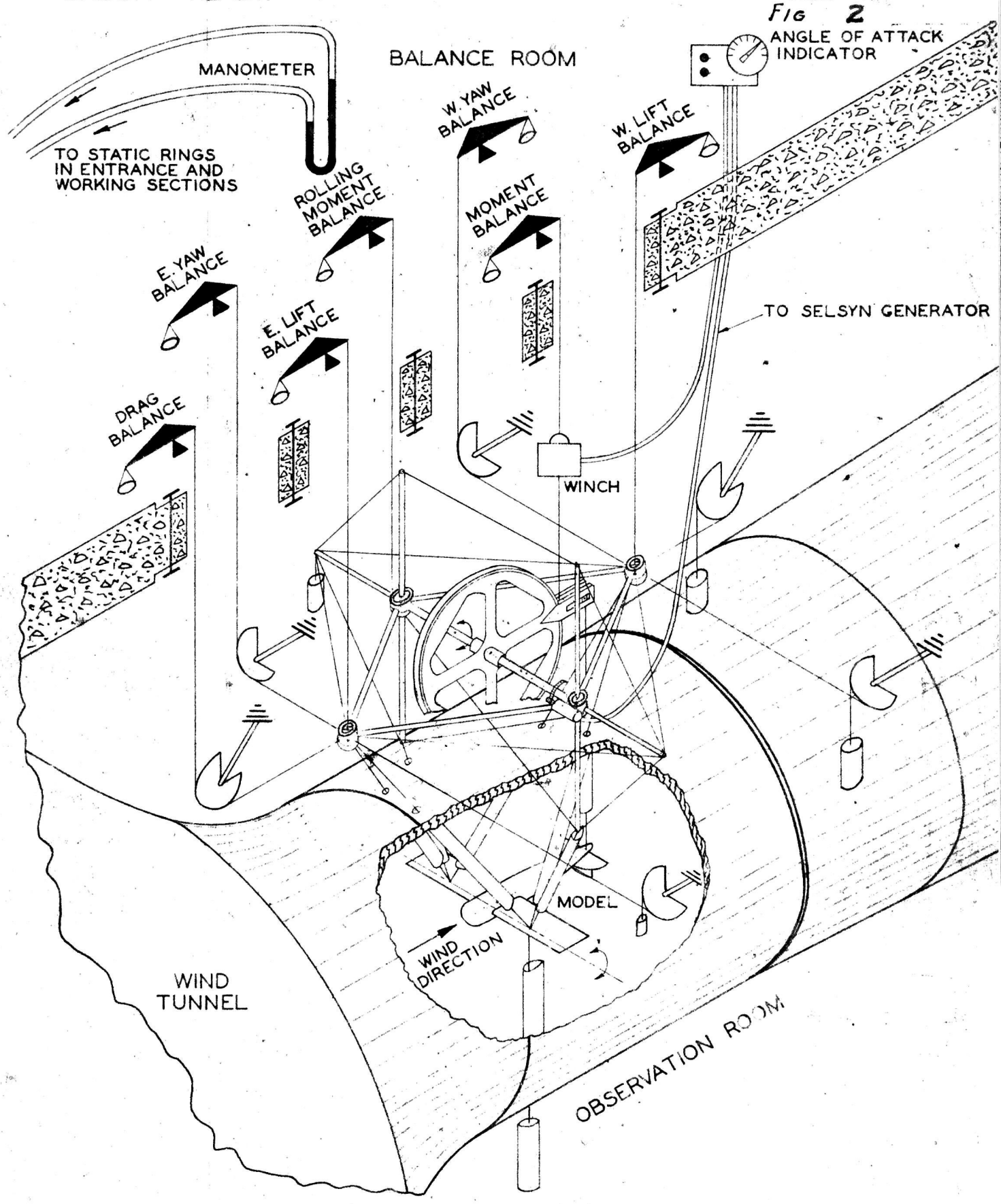

SIX COMPONENT SETUP FOR TEN FOOT WIND TUNNEL TESTS
AT GUGGENHEIM AERONAUTICS LABORATORY
CALIFORNIA INSTITUTE OF TECHNOLOGY

FIG

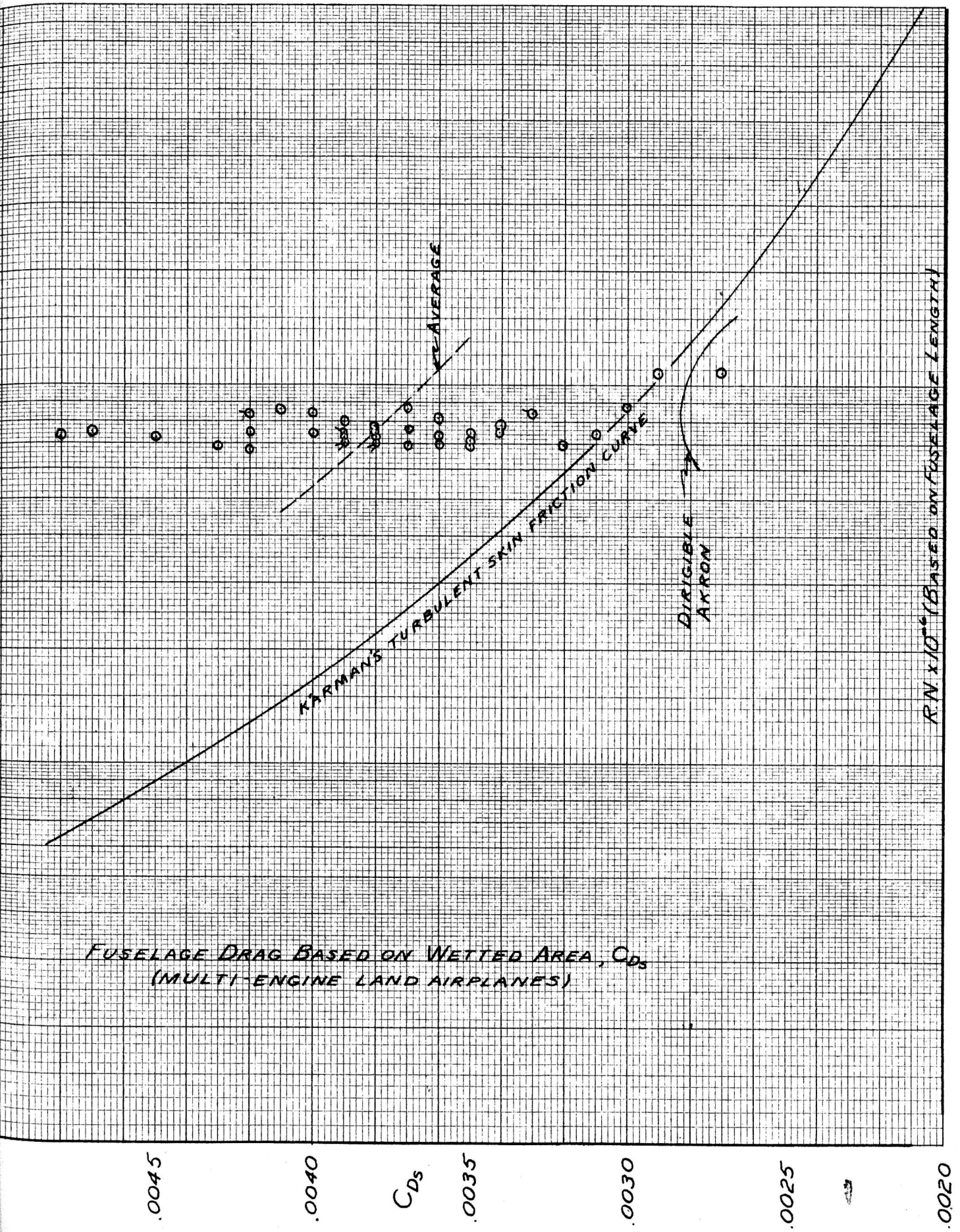
FUSELAGE DRAG BASED ON WETTED AREA, C_{D_S}
(MULTI-ENGINE LAND AIRPLANES)
C_{D_S}
.0045
.0040
.0035
.0030
.0025
.0020
R.N. x 10⁶ (BASED ON FUSELAGE LENGTH)
0.1
1.0
2.0
10.0
AVERAGE
KARMAN'S TURBULENT SKIN FRICTION CURVE
DIRIGIBLE
AKRON

C_{D_S} FOR TWO DIFFERENT TYPES OF CROSS-SECTIONS
WITH AND WITHOUT COCKPITS

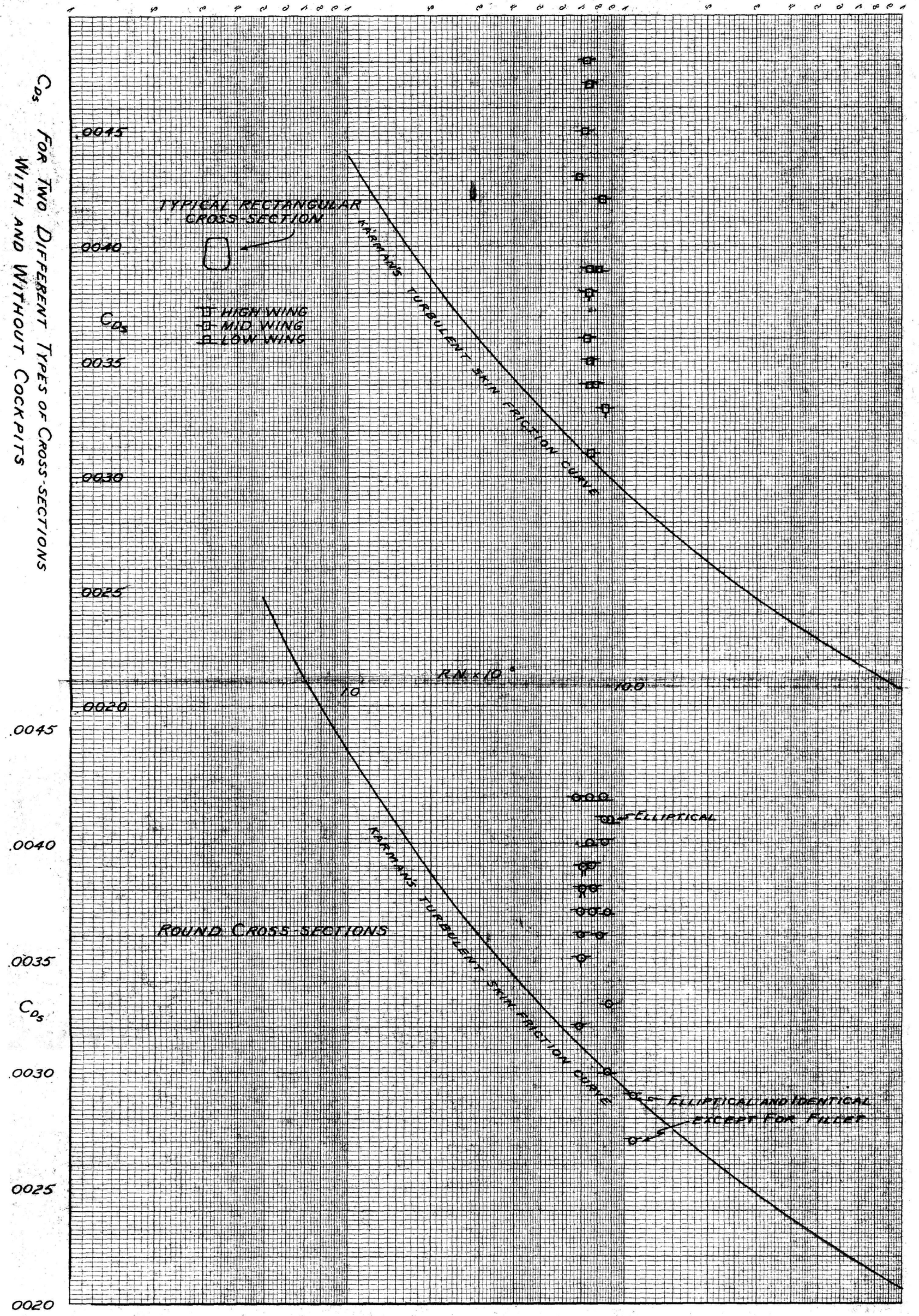

C_{D_s} FOR TWO DIFFERENT TYPES OF CROSS-SECTIONS WITHOUT COCKPITS

TYPICAL RECTANGULAR CROSS-SECTION

HIGH WING
MID WING
LOW WING

KÁRMÁN'S TURBULENT SKIN FRICTION CURVE

ROUND CROSS-SECTIONS

KÁRMÁN'S TURBULENT SKIN FRICTION CURVE

ELLIPTICAL AND IDENTICAL EXCEPT FOR FILLET

C_{D_s}

.0045
.0040
.0035
.0030
.0025
.0020

R.N. $\times 10^6$

0.1
1.0
10.0

R.N. $\times 10^{-6}$

FIG. 6

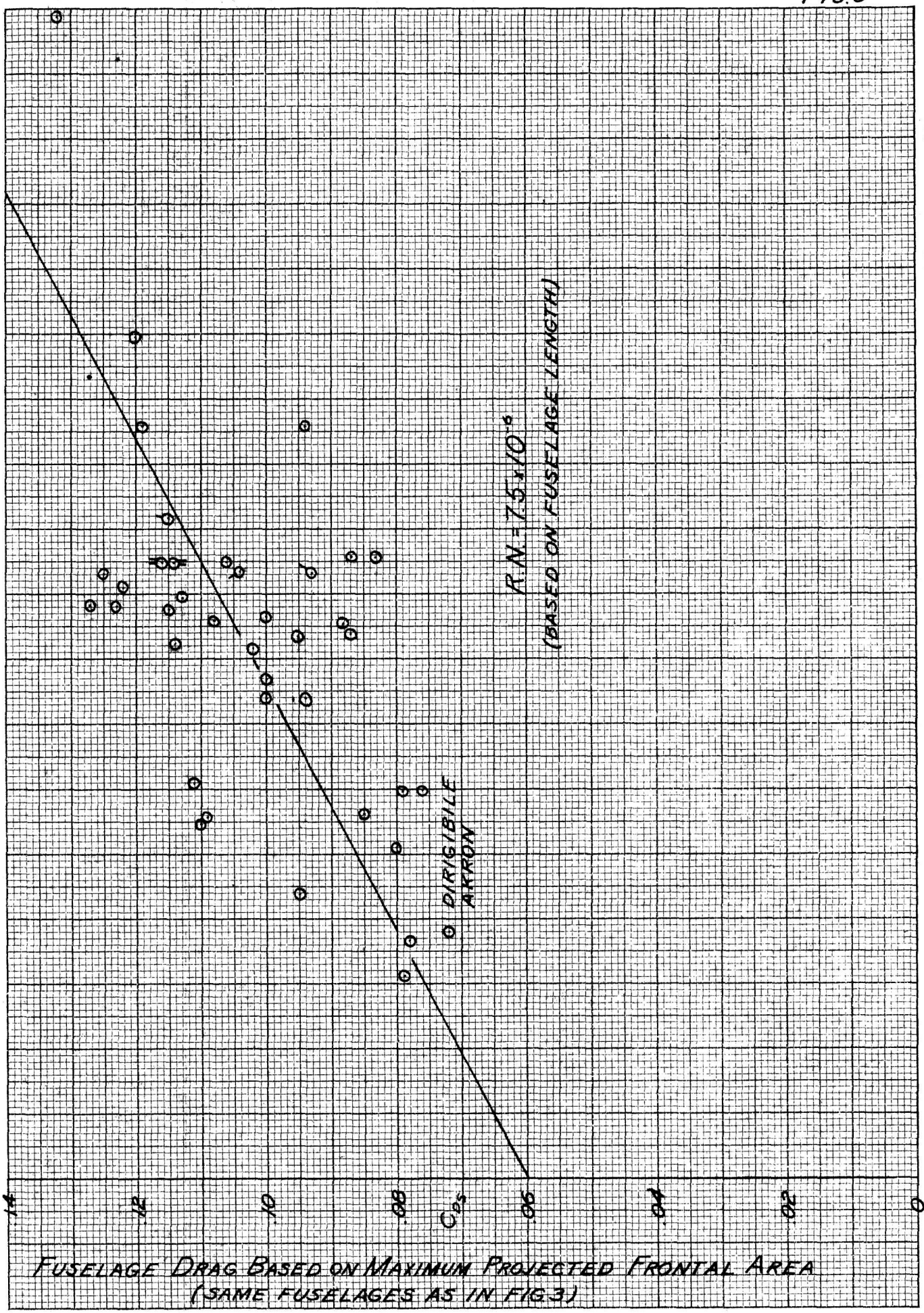

FUSELAGE DRAG BASED ON MAXIMUM PROJECTED FRONTAL AREA
(SAME FUSELAGES AS IN FIG 3)

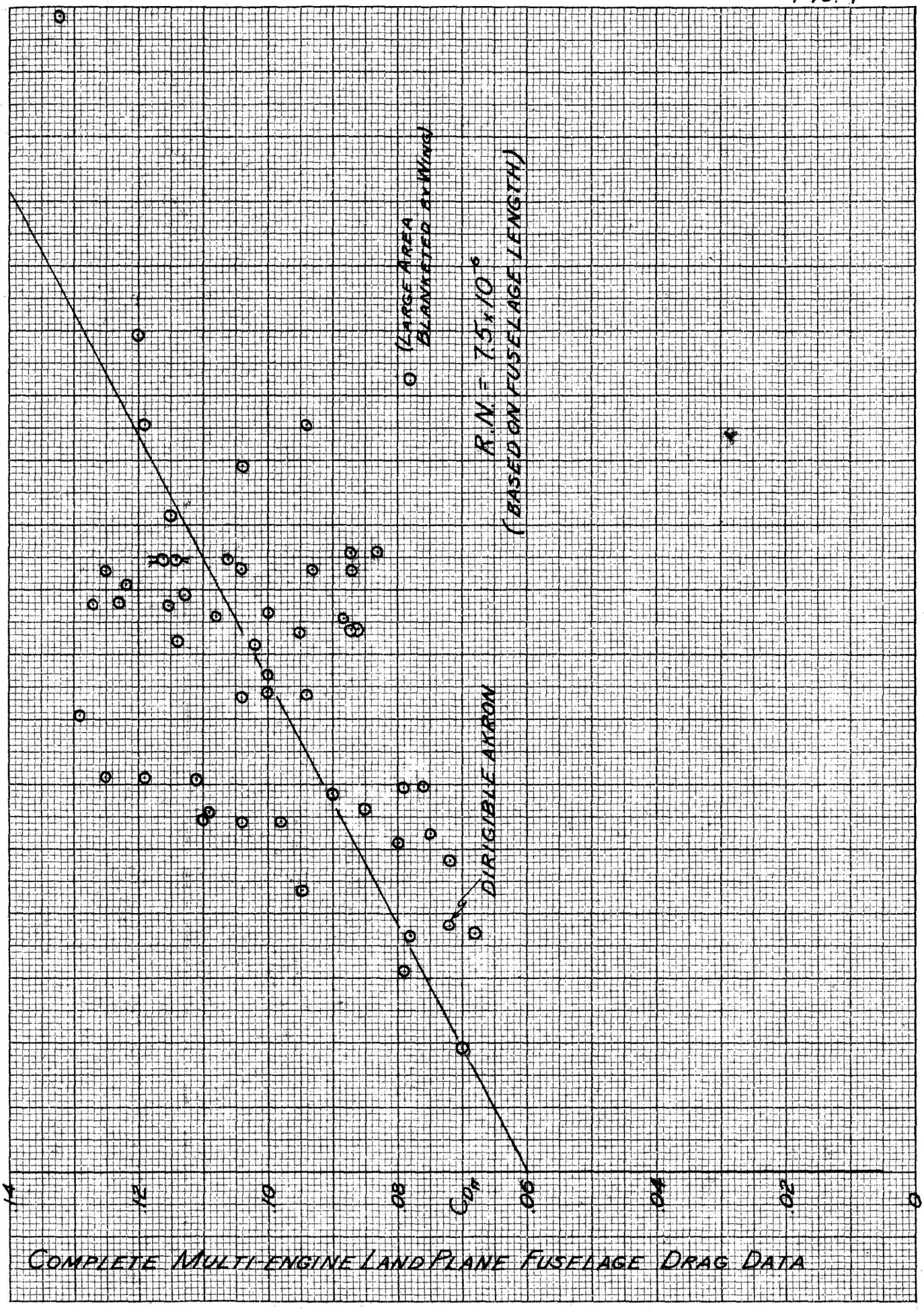

COMPLETE MULTI-ENGINE LAND PLANE FUSELAGE DRAG DATA

BREAKDOWN OF COMPLETE MULTI-ENGINE LAND PLANE FUSELAGE DRAG DATA

C_{D_N}

.12 .10 .08 .06

.12 .10 .08 .06

WITH AND WITHOUT COCKPIT

$R_N = 7.5 \times 10^6$

NO COCKPIT

ELLIPTICAL AND IDENTICAL EXCEPT FOR FILLET

DIRIGIBLE ARROW

ELLIPTICAL

WITH AND WITHOUT COCKPIT

$R_N = 7.5 \times 10^6$

NO COCKPIT

ELLIPTICAL AND IDENTICAL EXCEPT FOR FILLET

DIRIGIBLE ARROW

Similar for
- High Wing
- Mid Wing
- Low Wing

FINENESS RATIO

40 50 60 70 80 90 100 110 120

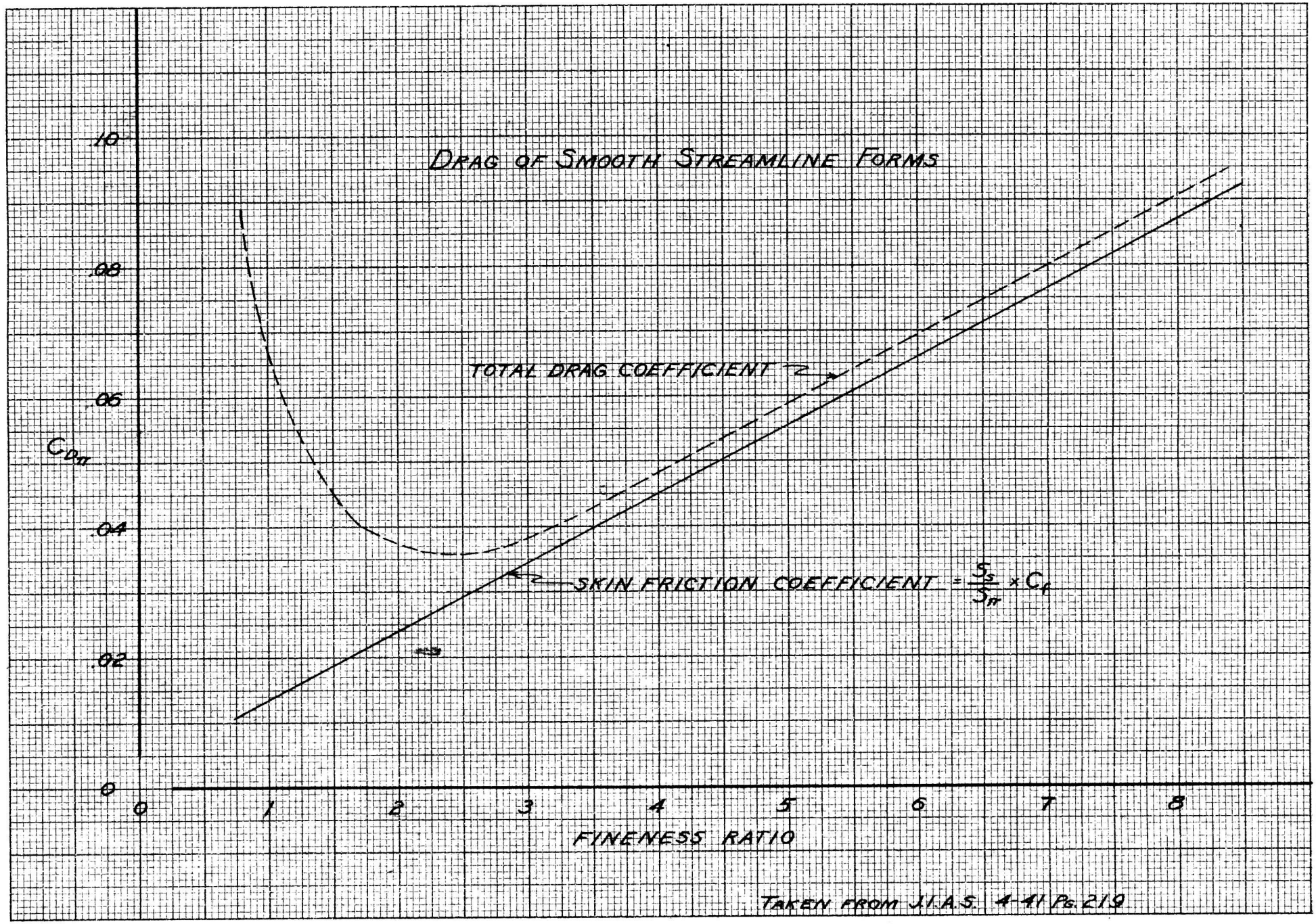
DRAG OF SMOOTH STREAMLINE FORMS
TOTAL DRAG COEFFICIENT
SKIN FRICTION COEFFICIENT = $\frac{S_s}{S_m} \times C_f$
C_{D_m}
.10
.08
.06
.04
.02
0
0
1
2
3
4
5
6
7
8
FINENESS RATIO
TAKEN FROM J.I.A.S. 4-41 PG. 219

PAGE 27
FIG. 9

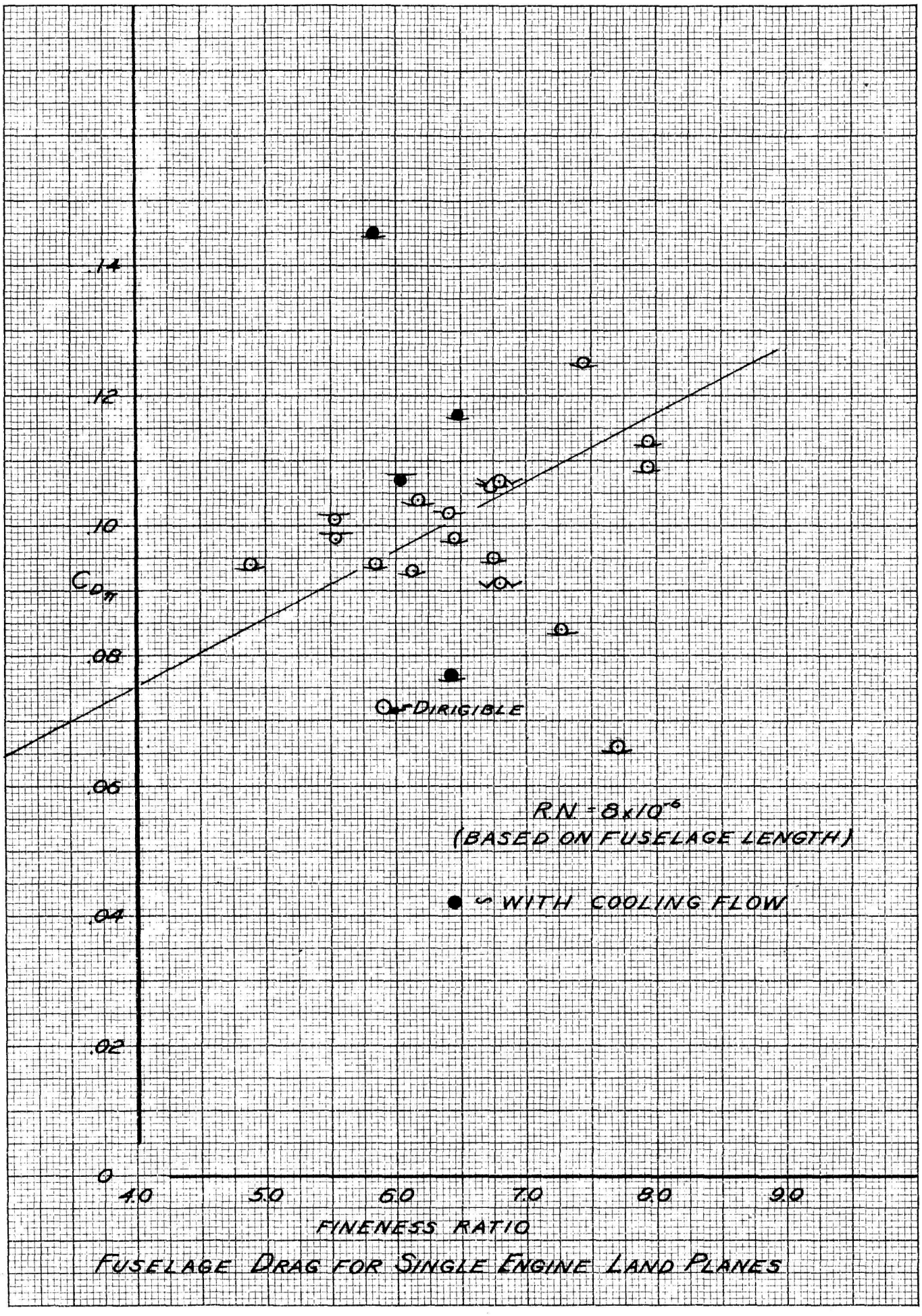

FUSELAGE DRAG FOR SINGLE ENGINE LAND PLANES

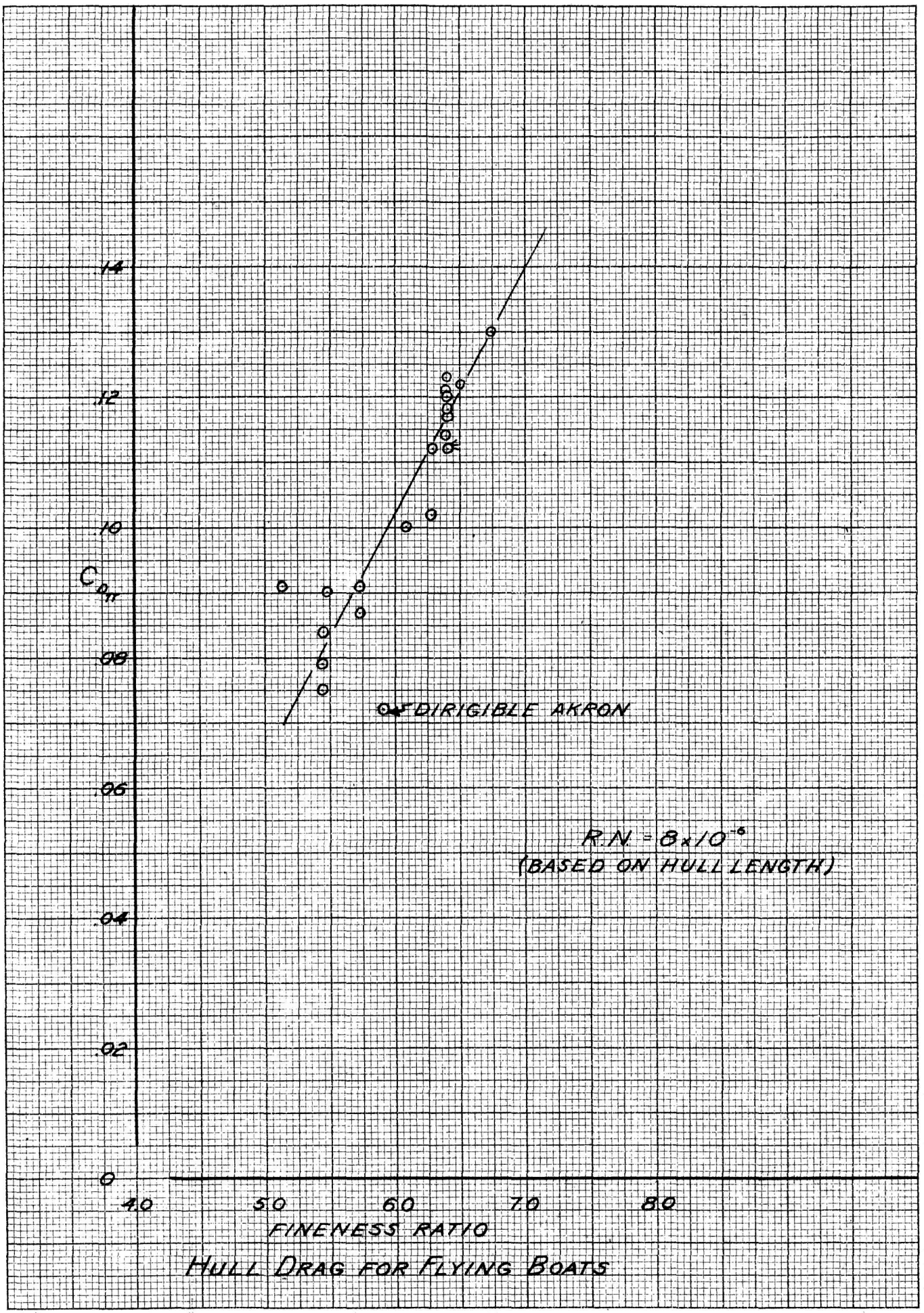

HULL DRAG FOR FLYING BOATS

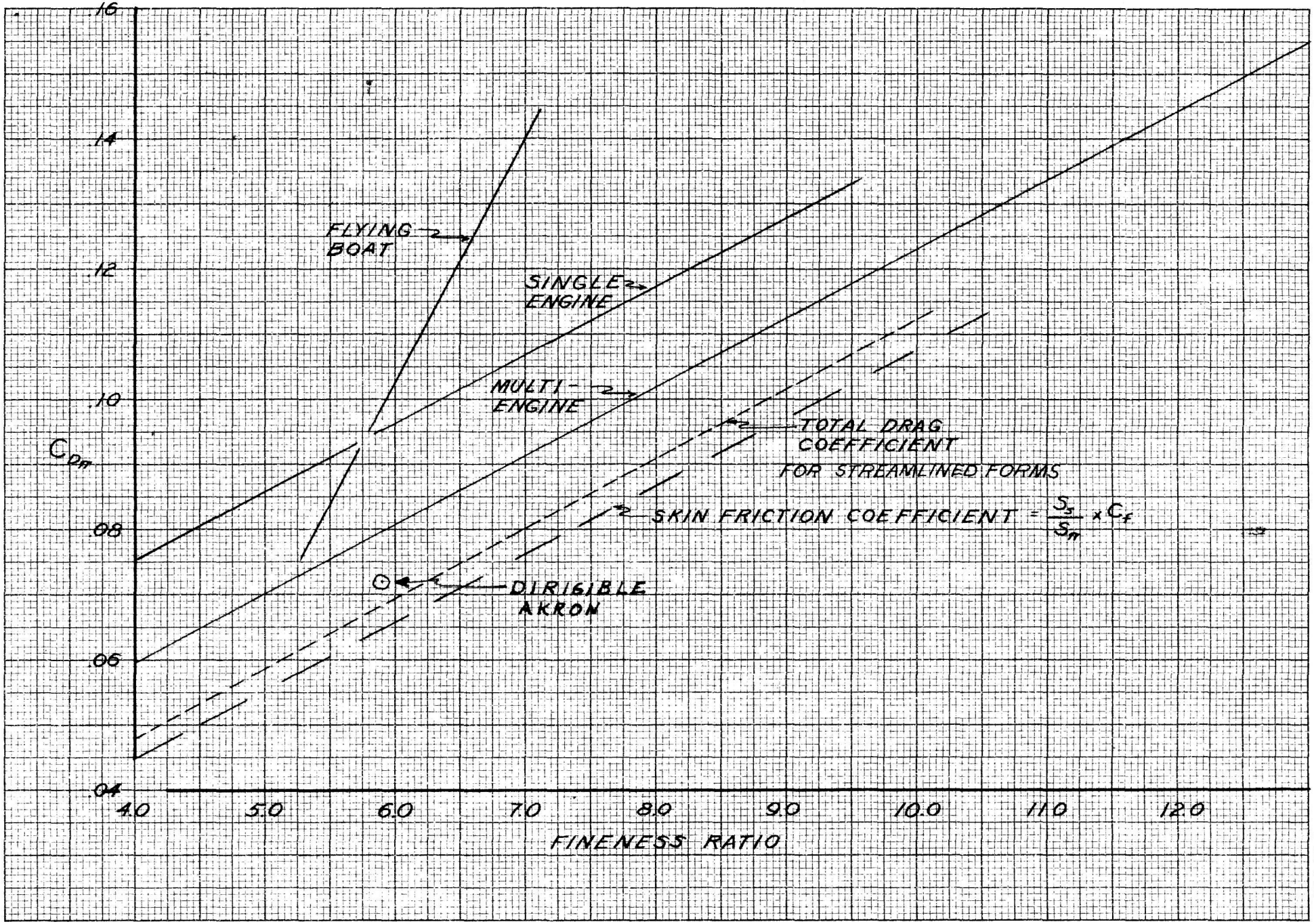
.16
.14
.12
.10
.08
.06
.04
C_{D_n}
FLYING BOAT
SINGLE ENGINE
MULTI-ENGINE
TOTAL DRAG COEFFICIENT FOR STREAMLINED FORMS
SKIN FRICTION COEFFICIENT = $\frac{S_s}{S_n} \times C_f$
DIRIGIBLE AKRON
4.0
5.0
6.0
7.0
8.0
9.0
10.0
11.0
12.0
FINENESS RATIO

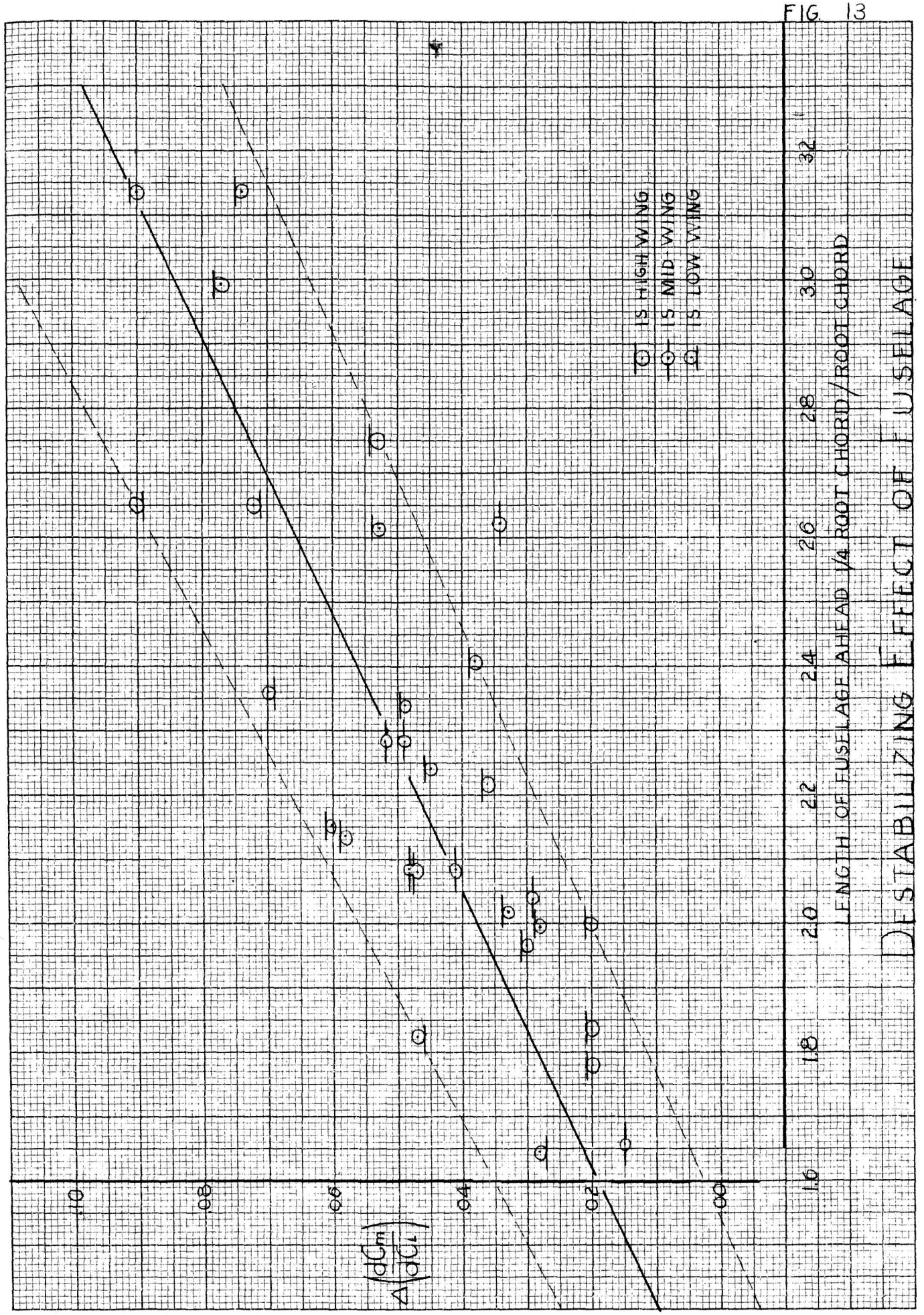
DESTABILIZING EFFECT OF FUSELAGE
LENGTH OF FUSELAGE AHEAD 1/4 ROOT CHORD/ROOT CHORD
1.6
1.8
2.0
2.2
2.4
2.6
2.8
3.0
3.2
$\Delta\left(\frac{dC_m}{dC_L}\right)$
.00
.02
.04
.06
.08
.10
IS HIGH WING
IS MID-WING
IS LOW WING

FIG. 14

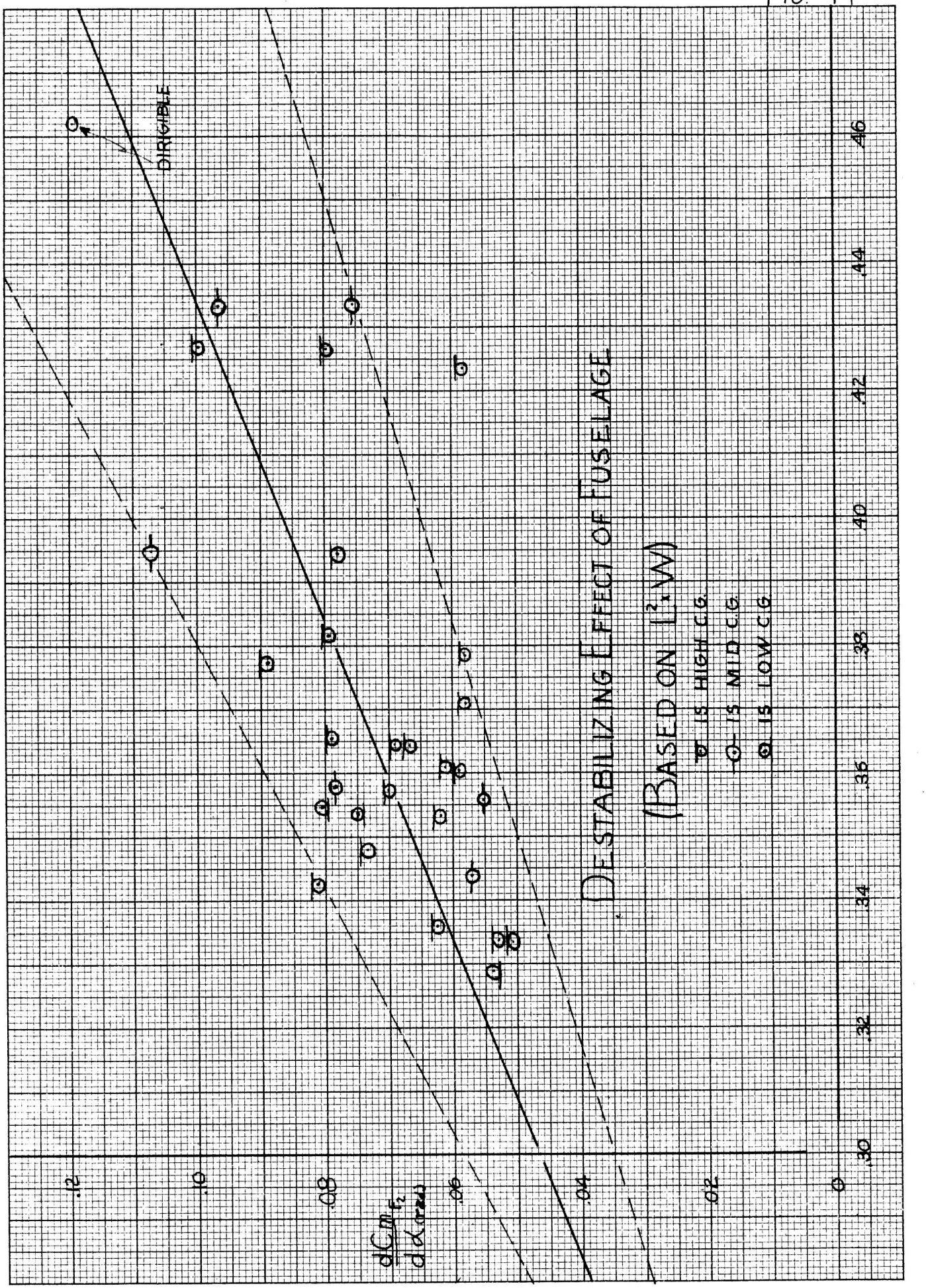
DIRIGIBLE
DESTABILIZING EFFECT OF FUSELAGE
(BASED ON $L^2 \times W$)
IS HIGH C.G.
IS MID C.G.
IS LOW C.G.
$\frac{dC_{m_{F_2}}}{d\alpha(rad)}$
.12
.10
.08
.06
.04
.02
0
.30
.32
.34
.36
.38
.40
.42
.44
.46

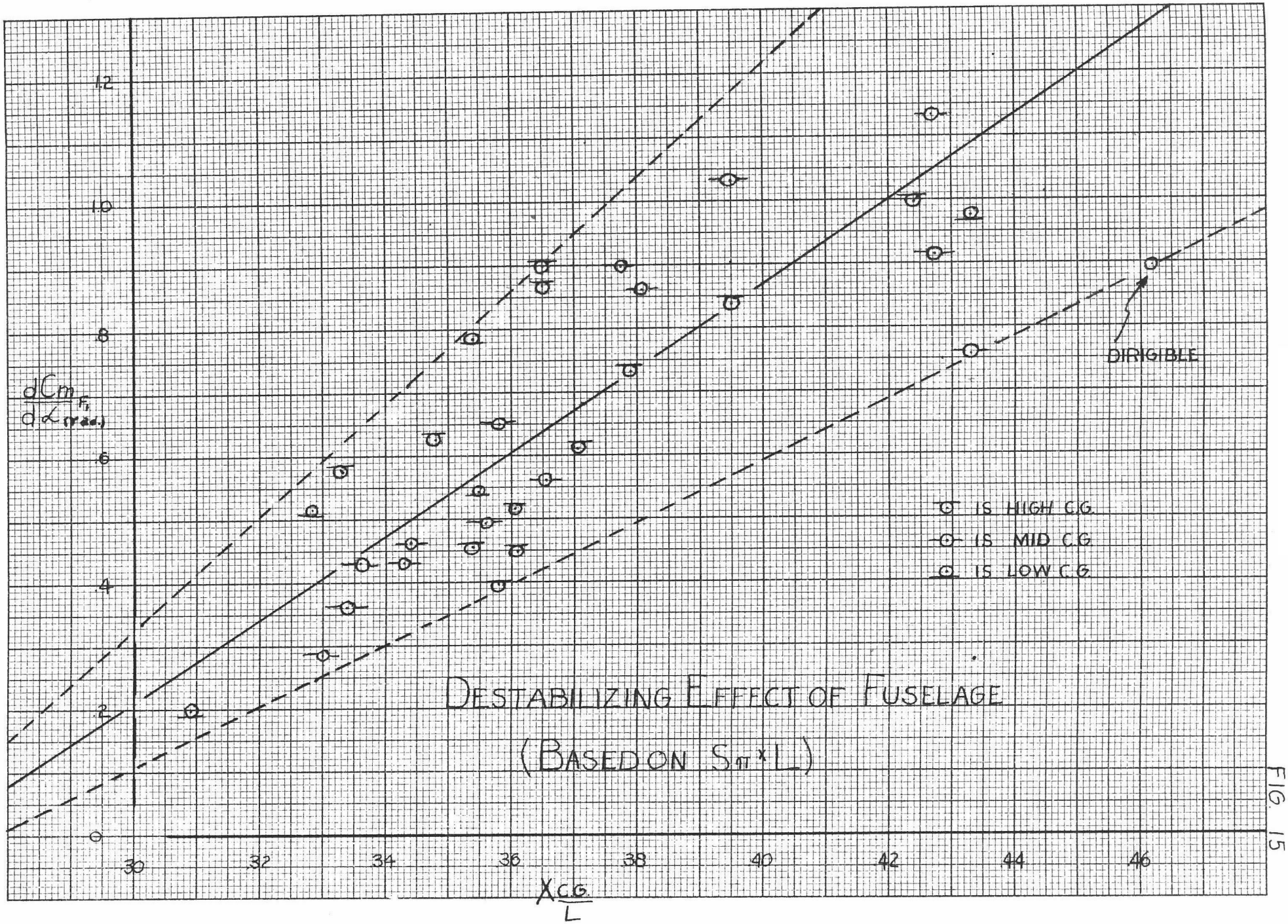
1.2
1.0
.8
.6
.4
.2
0
$\frac{dC_m}{d\alpha_{(rad.)}}$ F_1
30
32
34
36
38
40
42
44
46
$\frac{X_{C.G.}}{L}$
DIRIGIBLE
IS HIGH C.G.
IS MID C.G.
IS LOW C.G.
DESTABILIZING EFFECT OF FUSELAGE
(BASED ON $S_\pi \times L$)

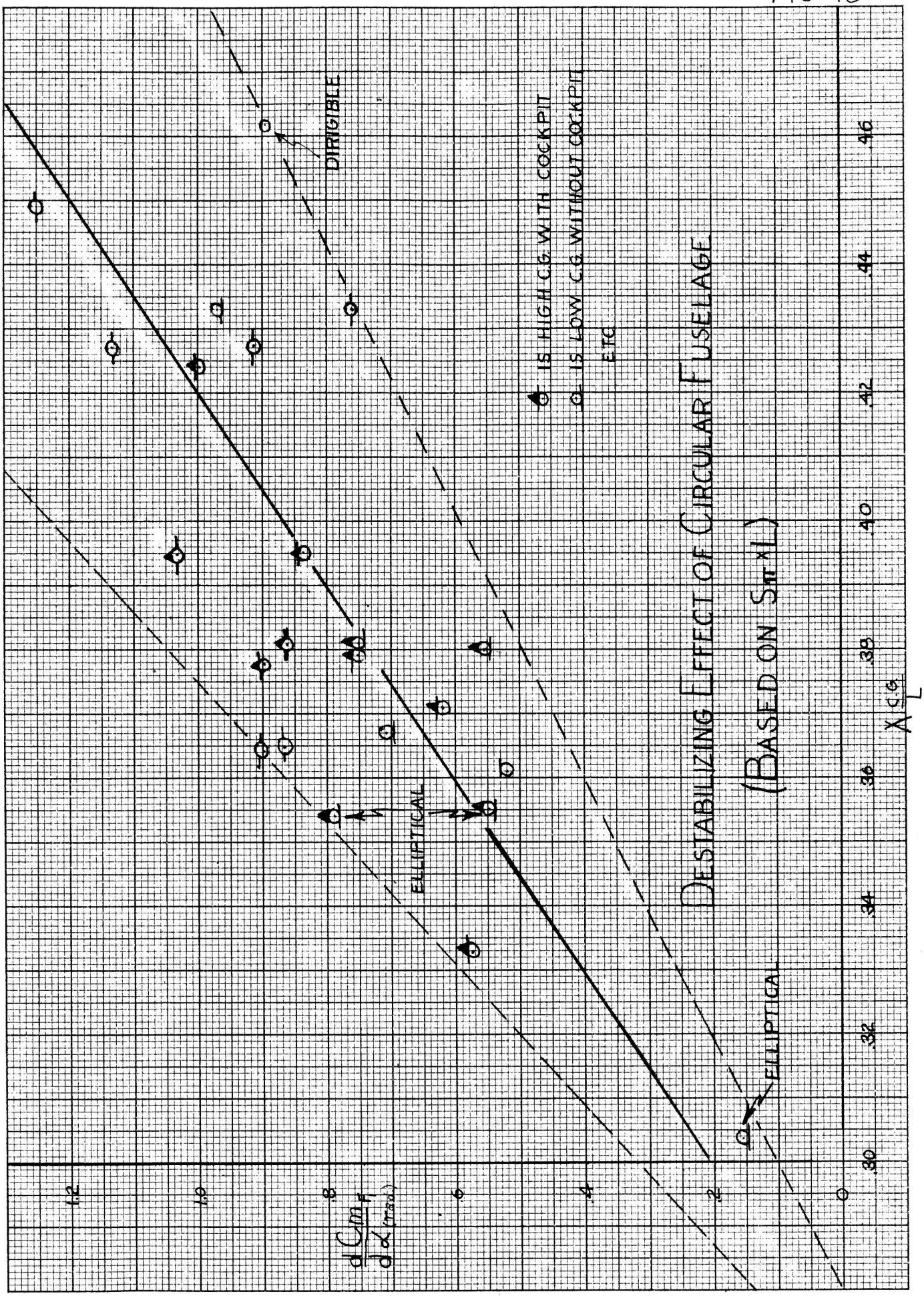
DESTABILIZING EFFECT OF CIRCULAR FUSELAGE
(BASED ON $S_{ft} \times L$)
DIRIGIBLE
ELLIPTICAL
ELLIPTICAL
IS HIGH C.G. WITH COCKPIT
IS LOW C.G. WITHOUT COCKPIT
ETC
$\frac{dC_{m_f}}{d\alpha\,(rad.)}$
1.2
1.0
.8
.6
.4
.2
0
.30
.32
.34
.36
.38
.40
.42
.44
.46
$X_{\frac{C.G.}{L}}$

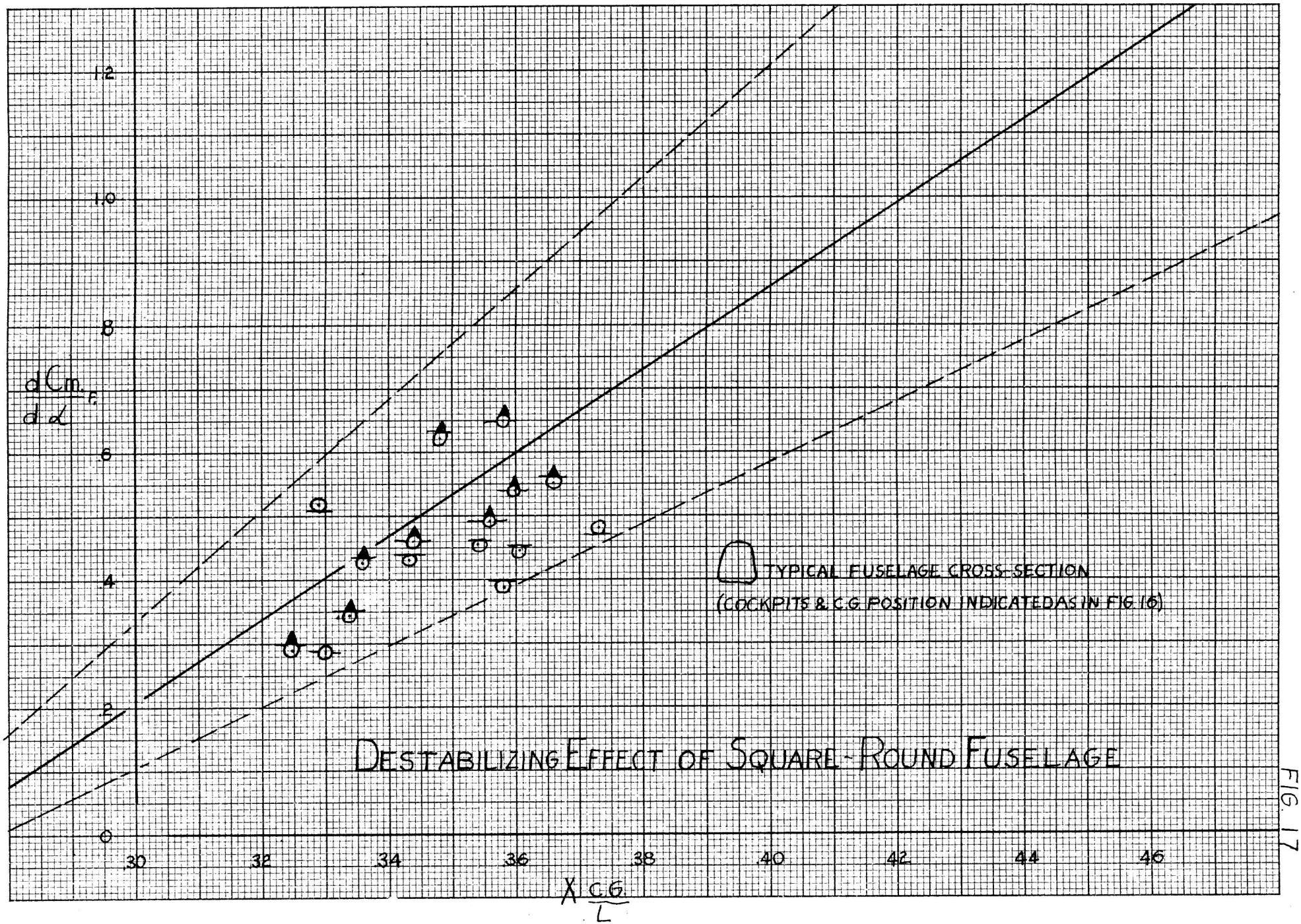

DESTABILIZING EFFECT OF SQUARE-ROUND FUSELAGE

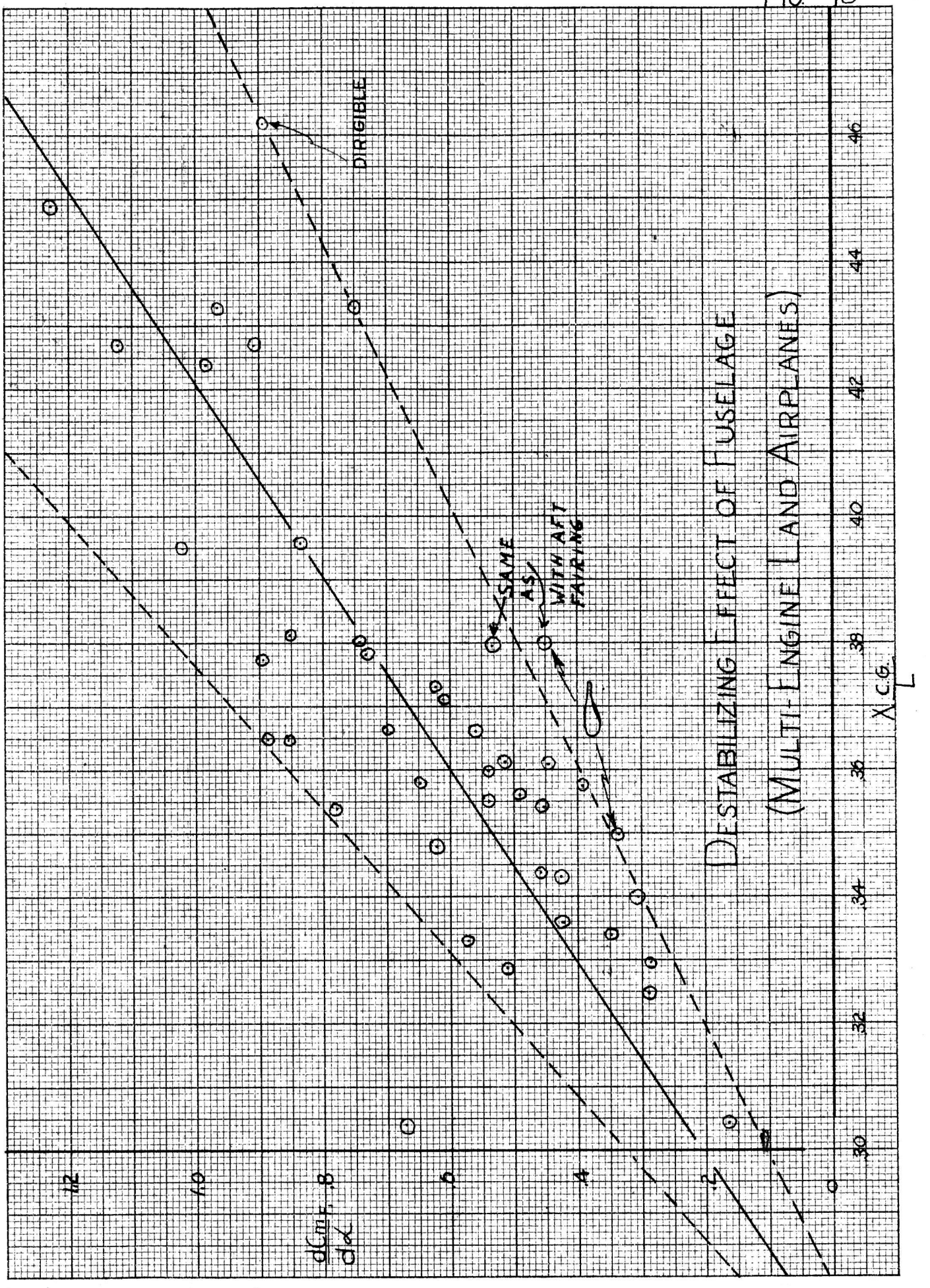
DESTABILIZING EFFECT OF FUSELAGE
(MULTI-ENGINE LAND AIRPLANES)
DIRIGIBLE
SAME AS WITH AFT FAIRING
$\frac{d C_{m_F}}{d \alpha} \cdot 8$
$\bar{\chi}$ c.g.
12
10
8
6
4
2
0
30
32
34
36
38
40
42
44
46

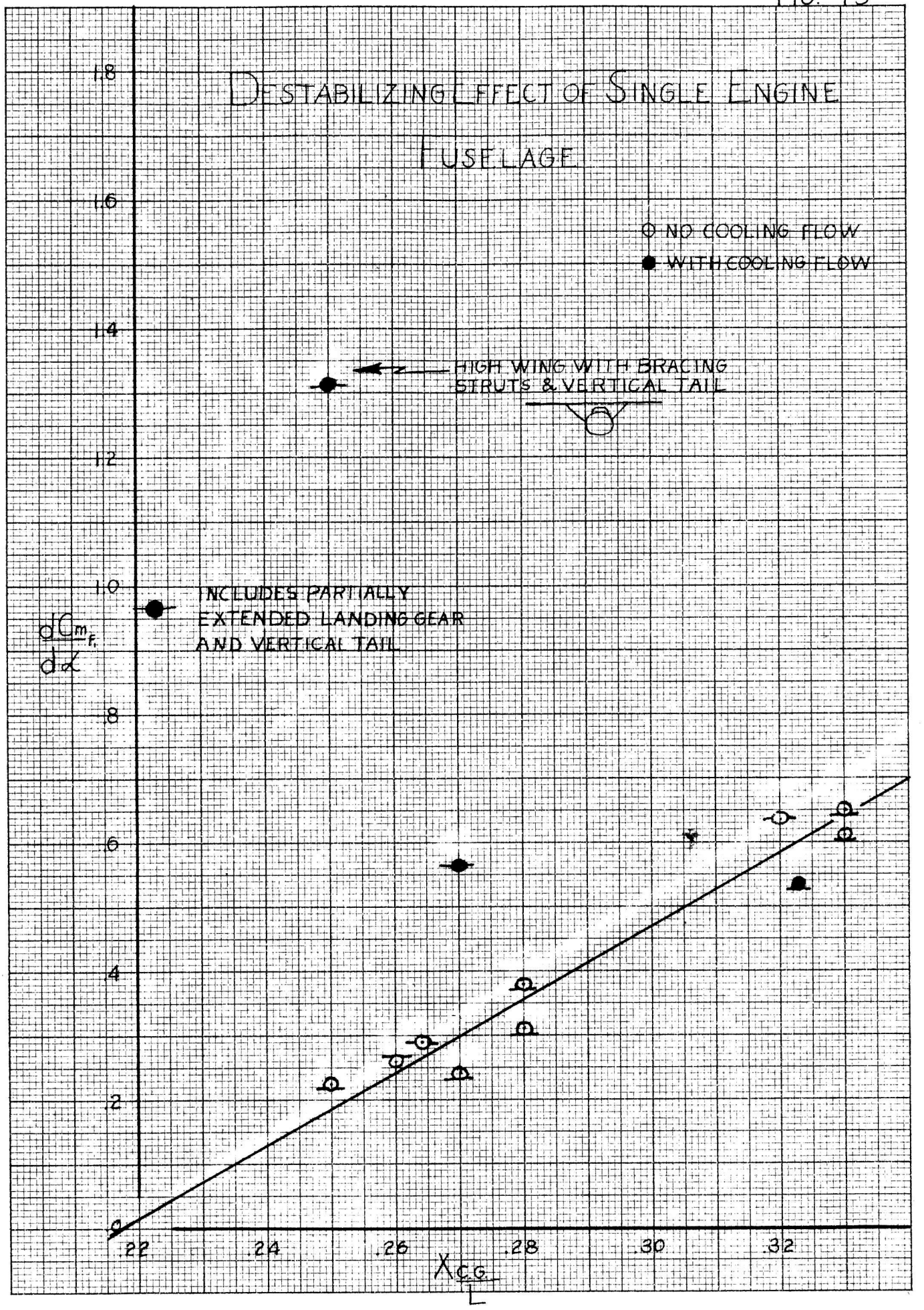
DESTABILIZING EFFECT OF SINGLE ENGINE FUSELAGE
NO COOLING FLOW
WITH COOLING FLOW
HIGH WING WITH BRACING STRUTS & VERTICAL TAIL
INCLUDES PARTIALLY EXTENDED LANDING GEAR AND VERTICAL TAIL
dCm f. / dα
1.8
1.6
1.4
1.2
1.0
.8
.6
.4
.2
0
.22
.24
.26
.28
.30
.32
XC.G. / L

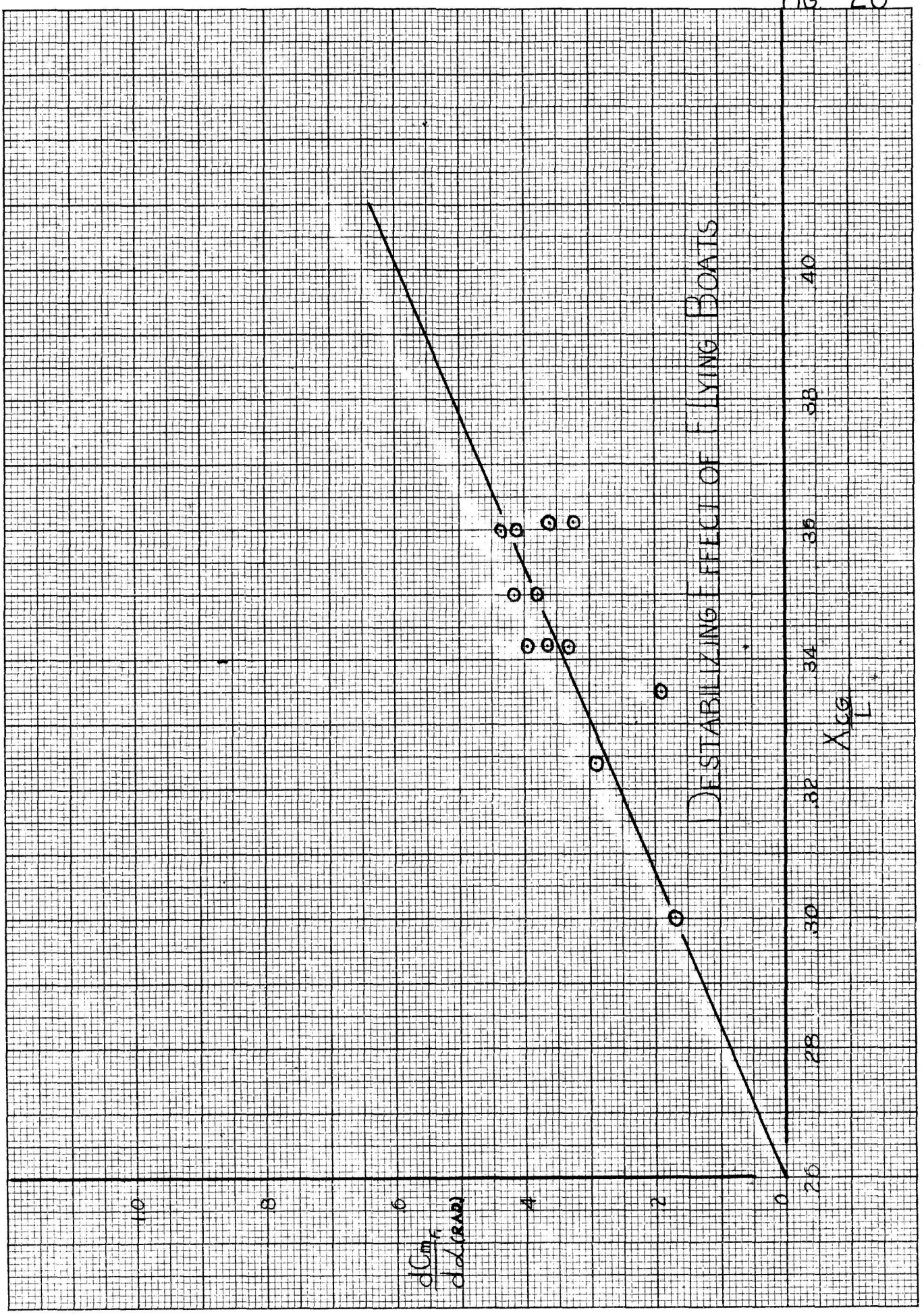
DESTABILIZING EFFECT OF FLYING BOATS
$\frac{dC_{m_F}}{d\alpha_{(RAD)}}$
10
8
6
4
2
0
26
28
30
32
34
36
38
40
X_{CG}

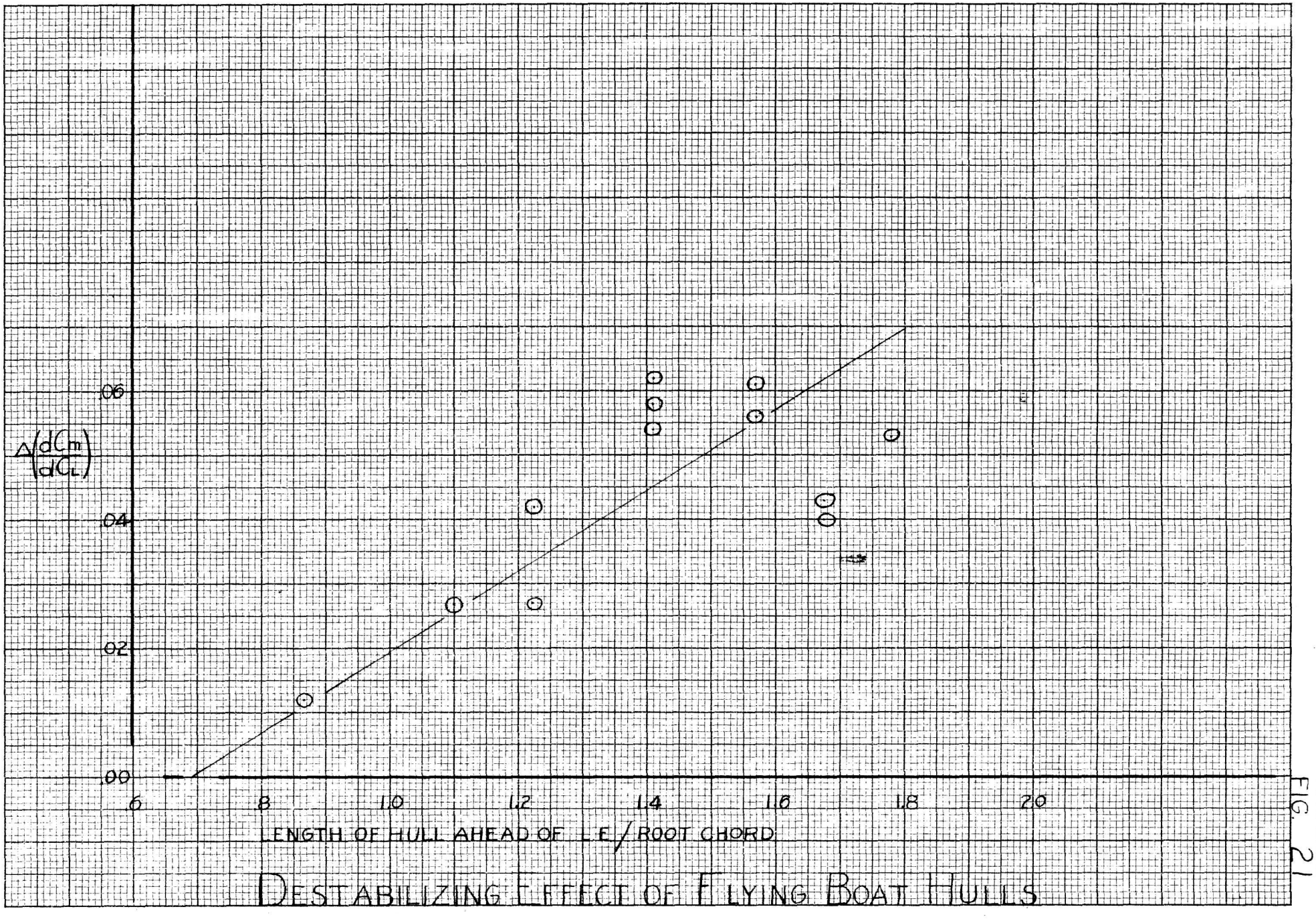

DESTABILIZING EFFECT OF FLYING BOAT HULLS

PAGE 39
FIG. 21

FIG. 22

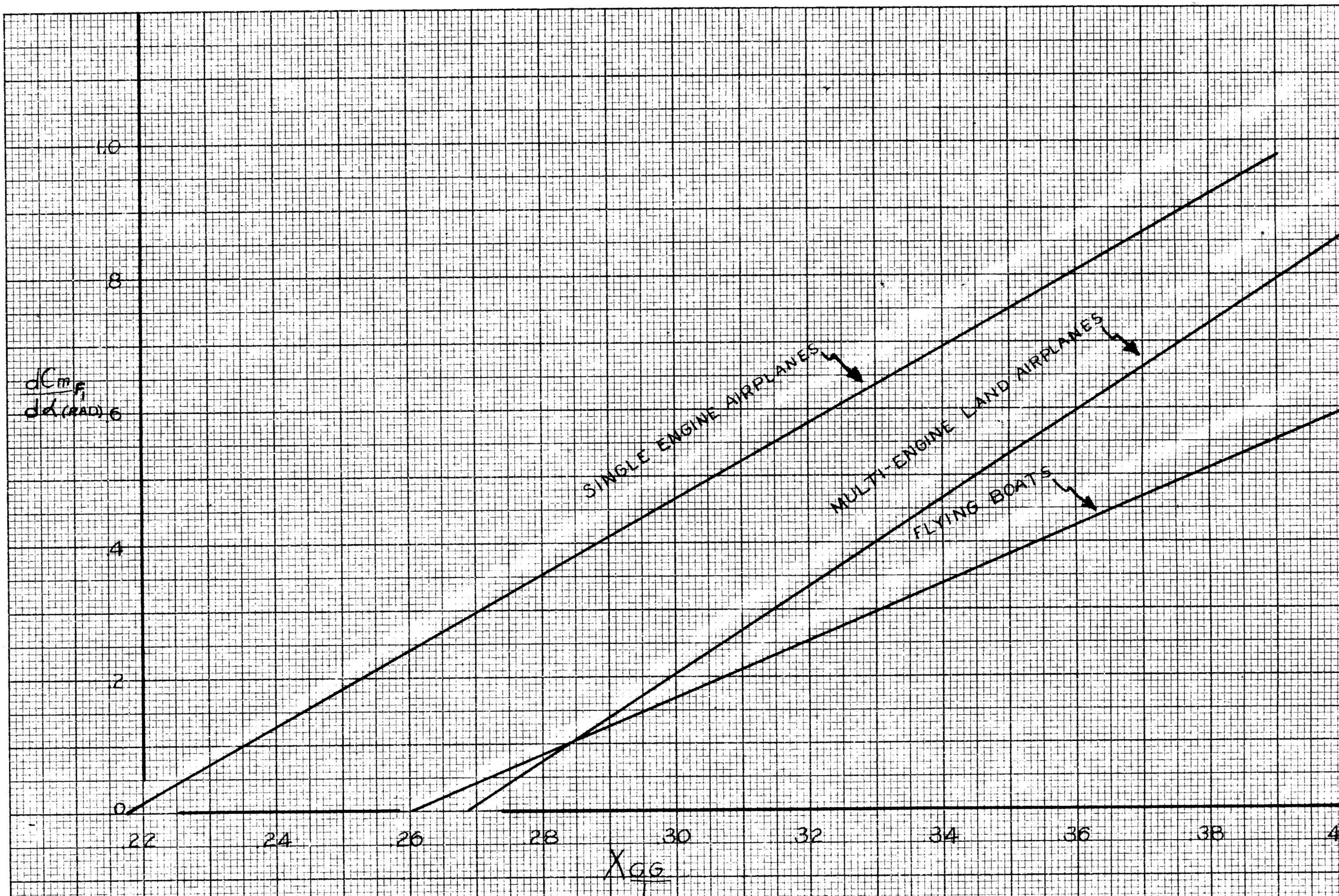

DESTABILIZING EFFECT OF FUSELAGES AND FLYING BOAT HULLS

FIG 23

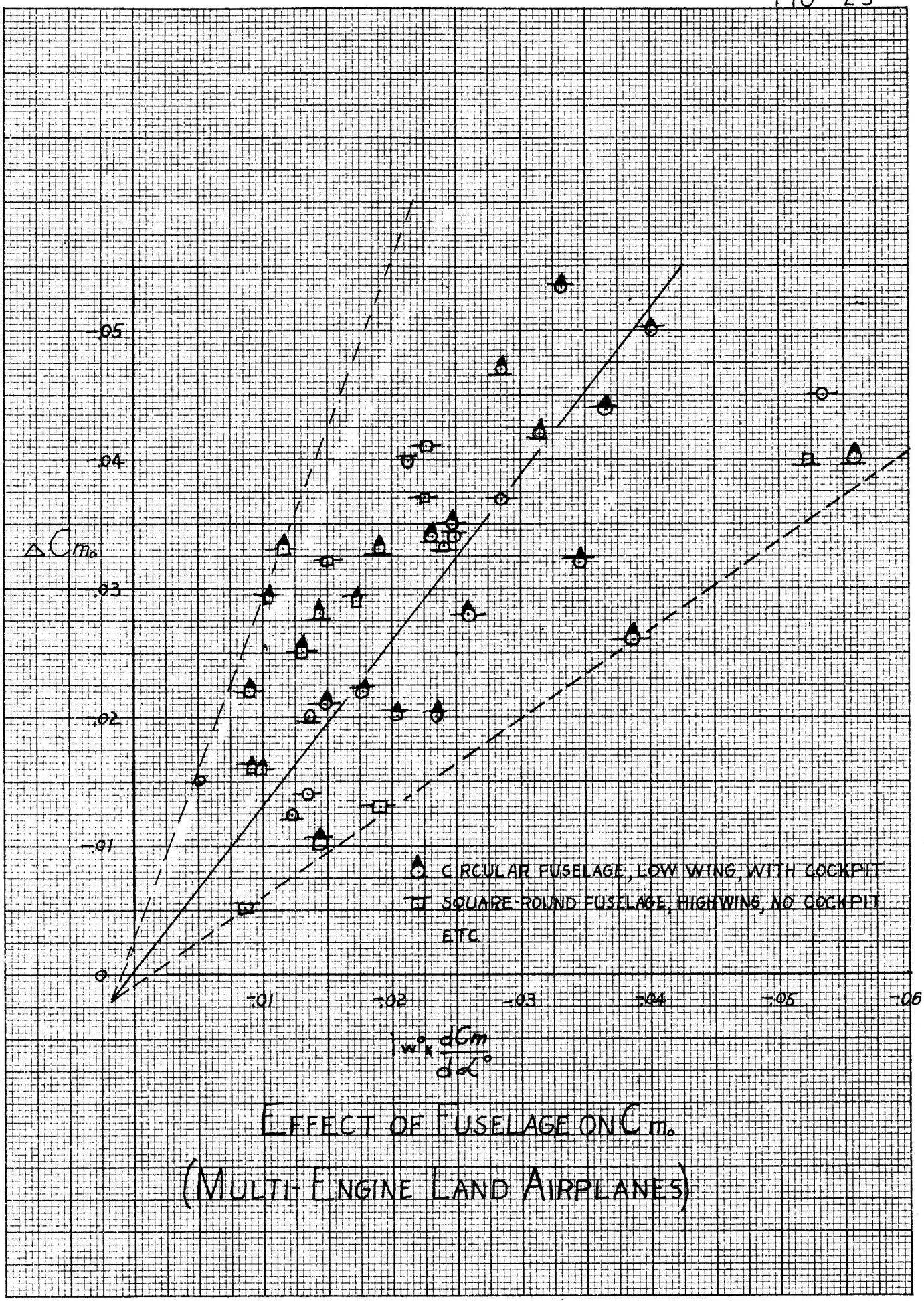

EFFECT OF FUSELAGE ON C_{m_o}

(MULTI-ENGINE LAND AIRPLANES)

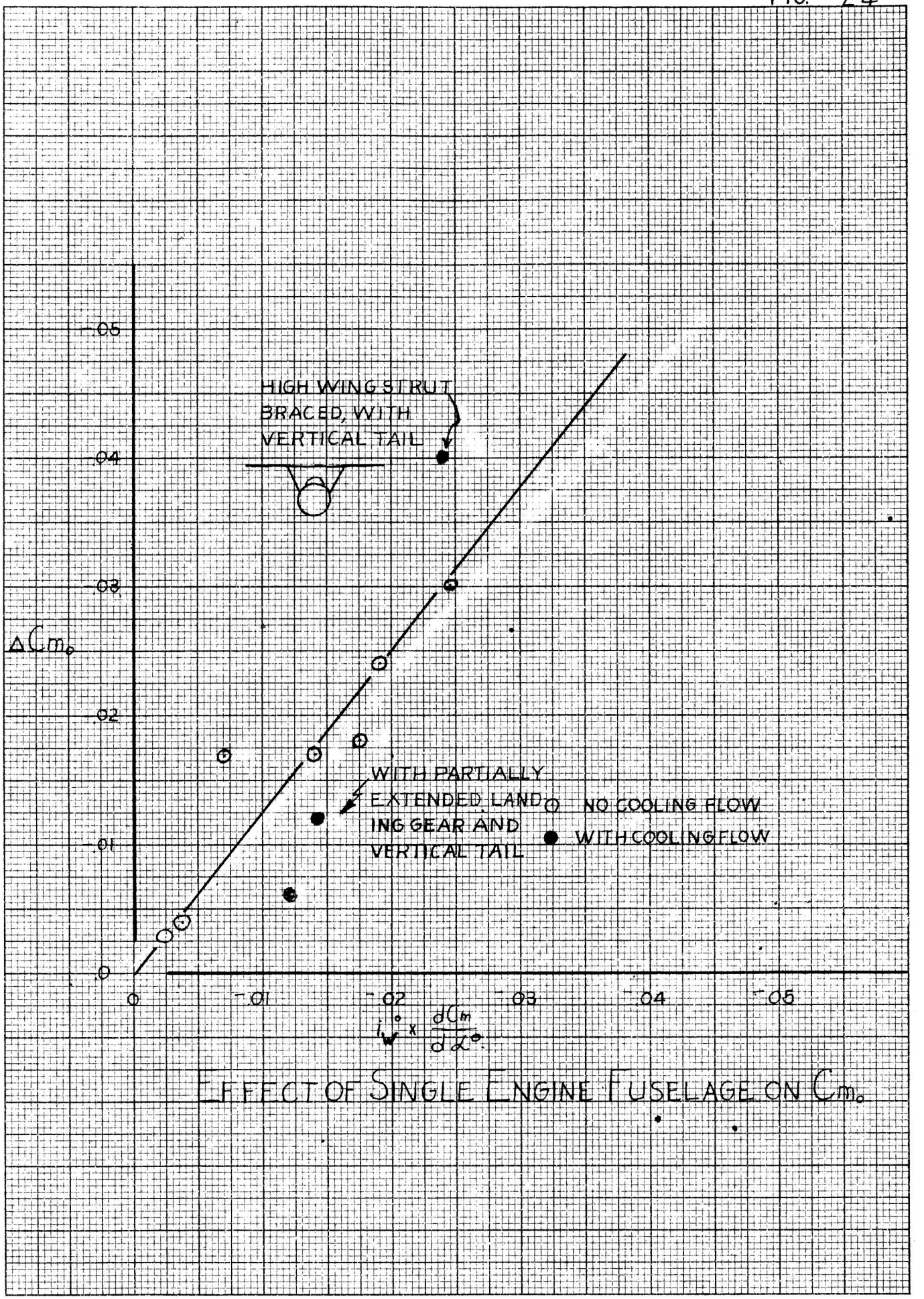

EFFECT OF SINGLE ENGINE FUSELAGE ON C_{m_0}

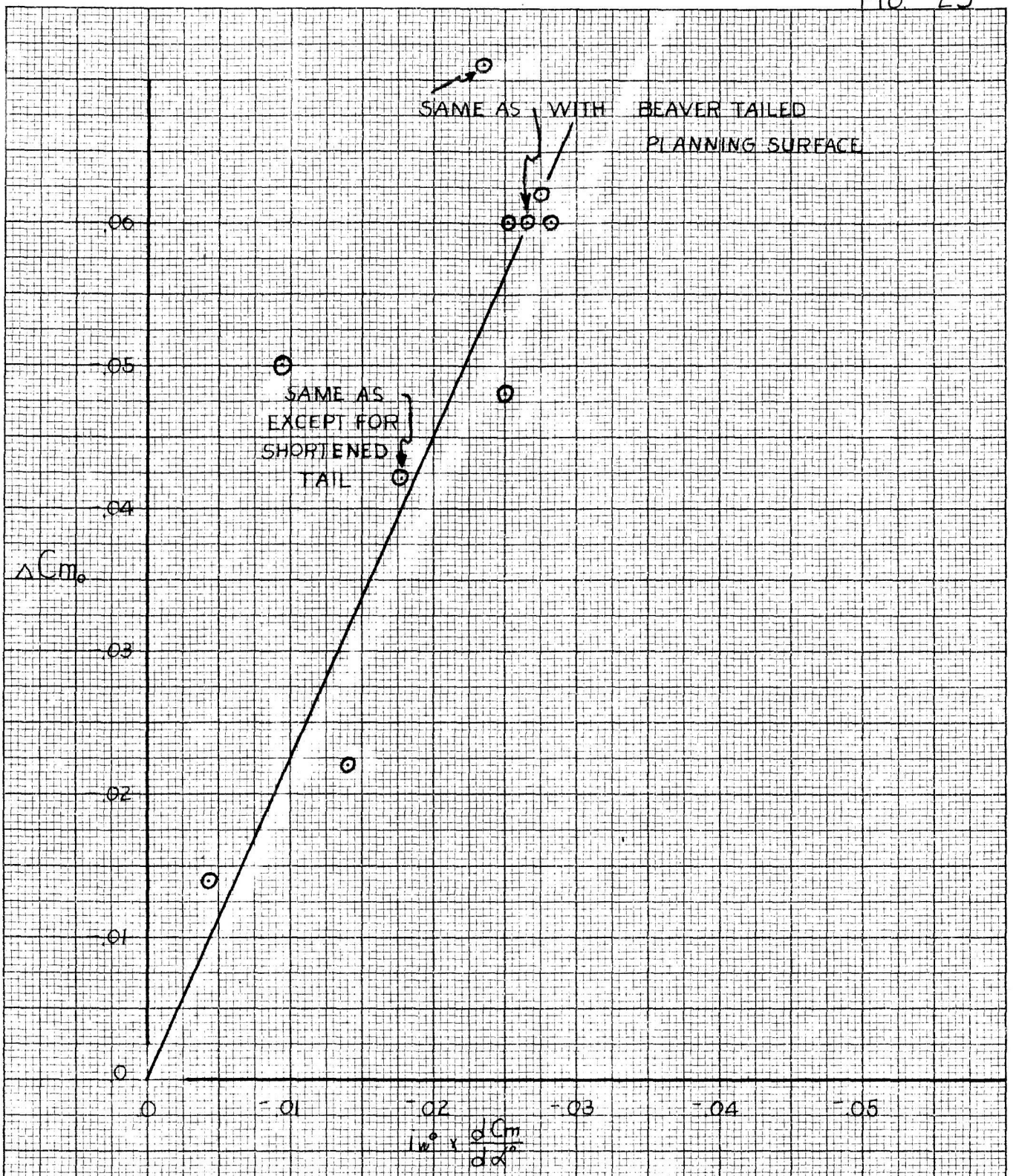

EFFECT OF FLYING BOAT HULLS ON C_{m_0}

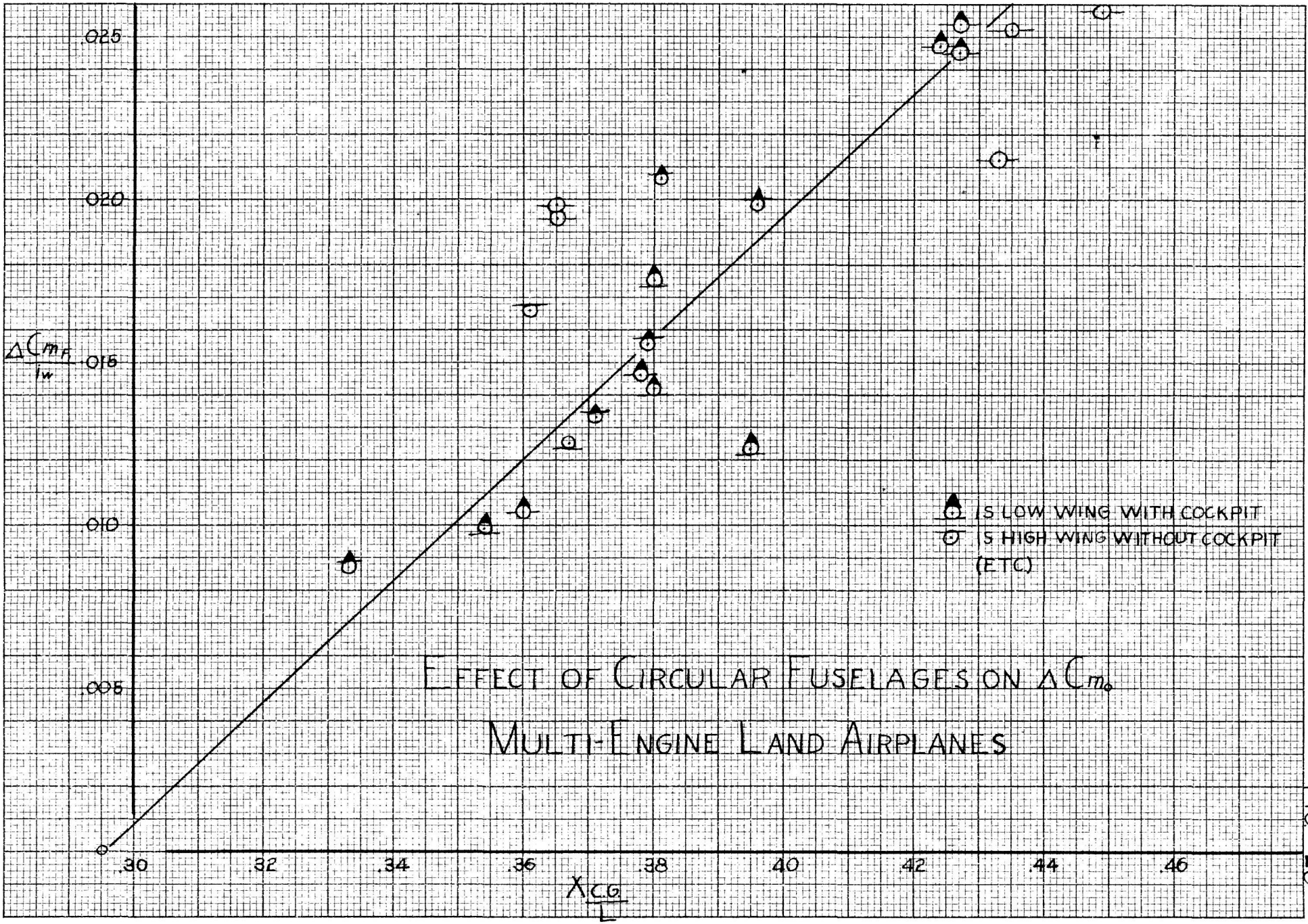

EFFECT OF CIRCULAR FUSELAGES ON ΔC_{m_o}

MULTI-ENGINE LAND AIRPLANES

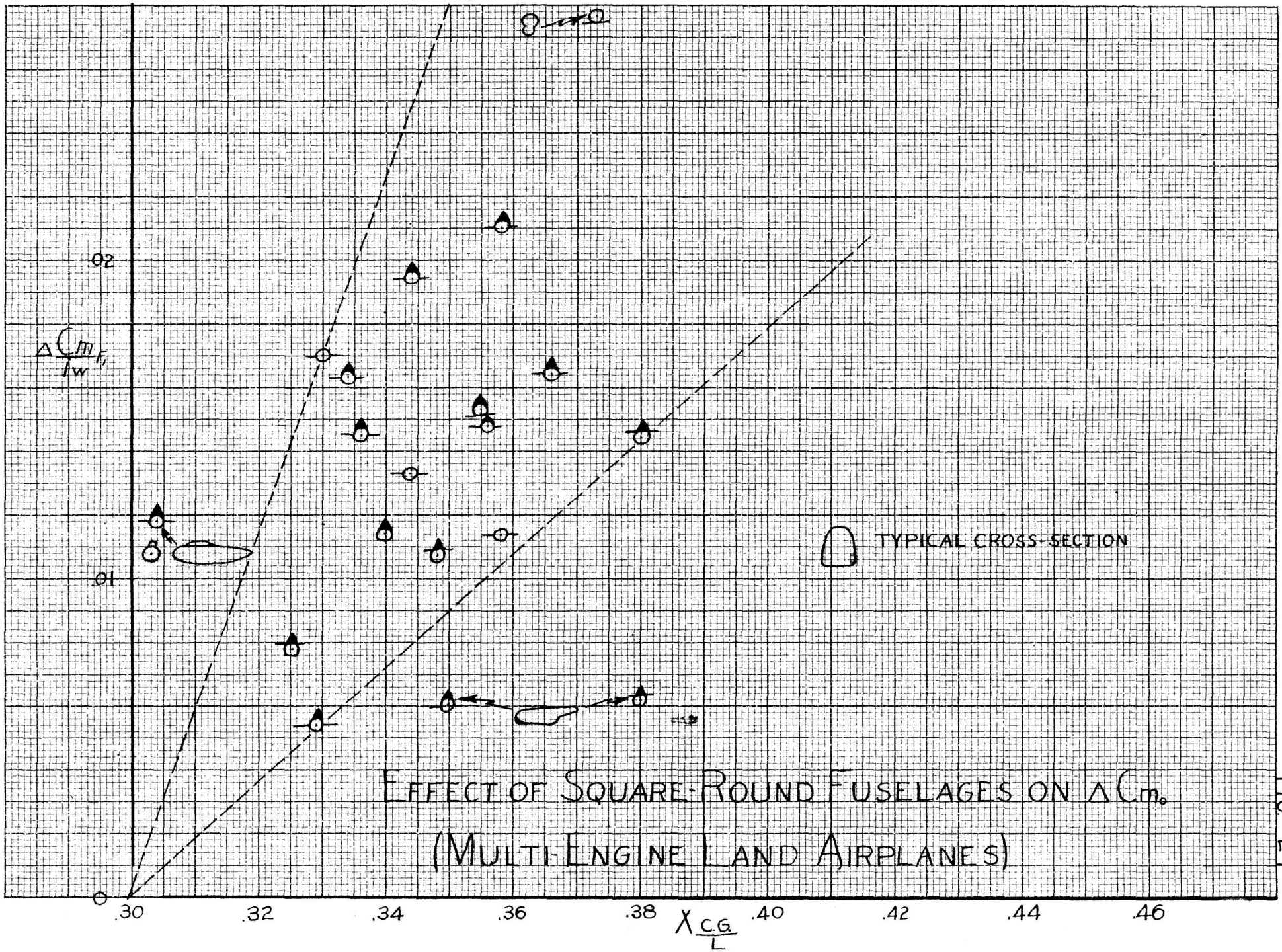

EFFECT OF SQUARE-ROUND FUSELAGES ON ΔC_{m_o}
(MULTI-ENGINE LAND AIRPLANES)

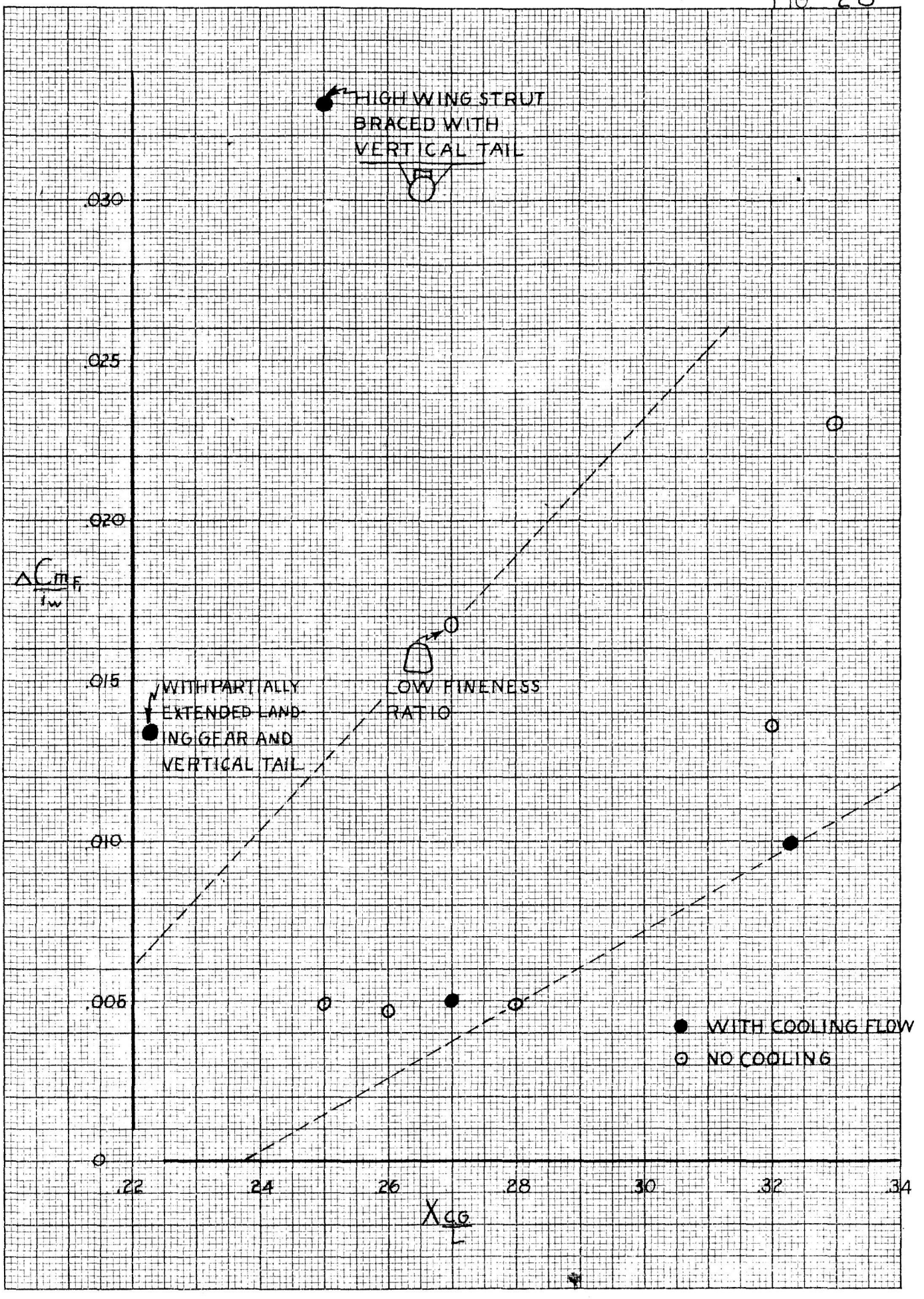
HIGH WING STRUT BRACED WITH VERTICAL TAIL
.030
.025
.020
$\Delta C_{m_{F_i}}$
i_w
.015
WITH PARTIALLY EXTENDED LANDING GEAR AND VERTICAL TAIL
LOW FINENESS RATIO
.010
.005
0
.22
.24
.26
.28
.30
.32
.34
$X_{\frac{CG}{L}}$
WITH COOLING FLOW
NO COOLING

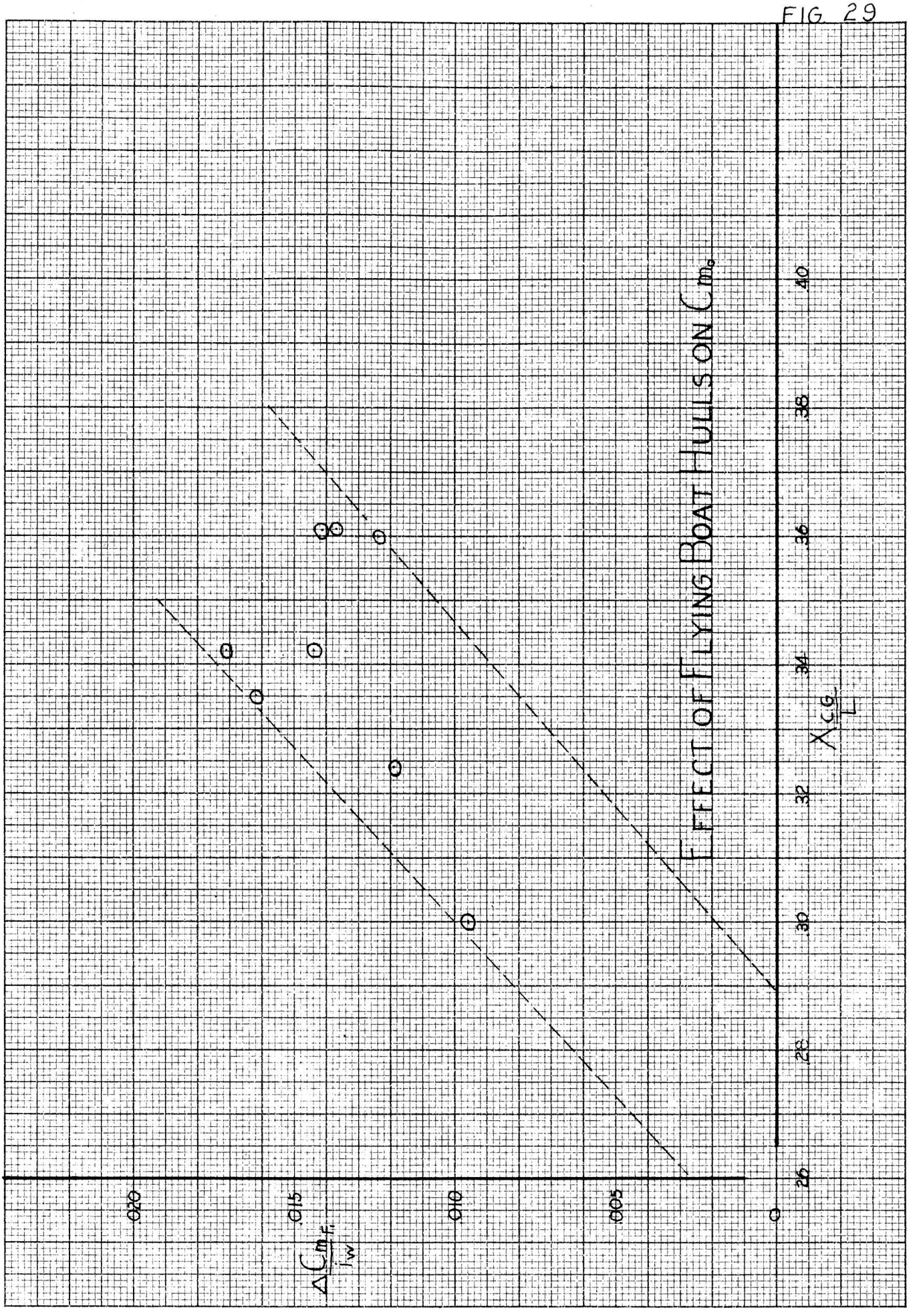
EFFECT OF FLYING BOAT HULLS ON C_{m_o}
$\Delta C_{m_{F.F.}}$
i_w
.020
.015
.010
.005
0
26
28
30
32
34
36
38
40
$\frac{X_{C.G.}}{L}$

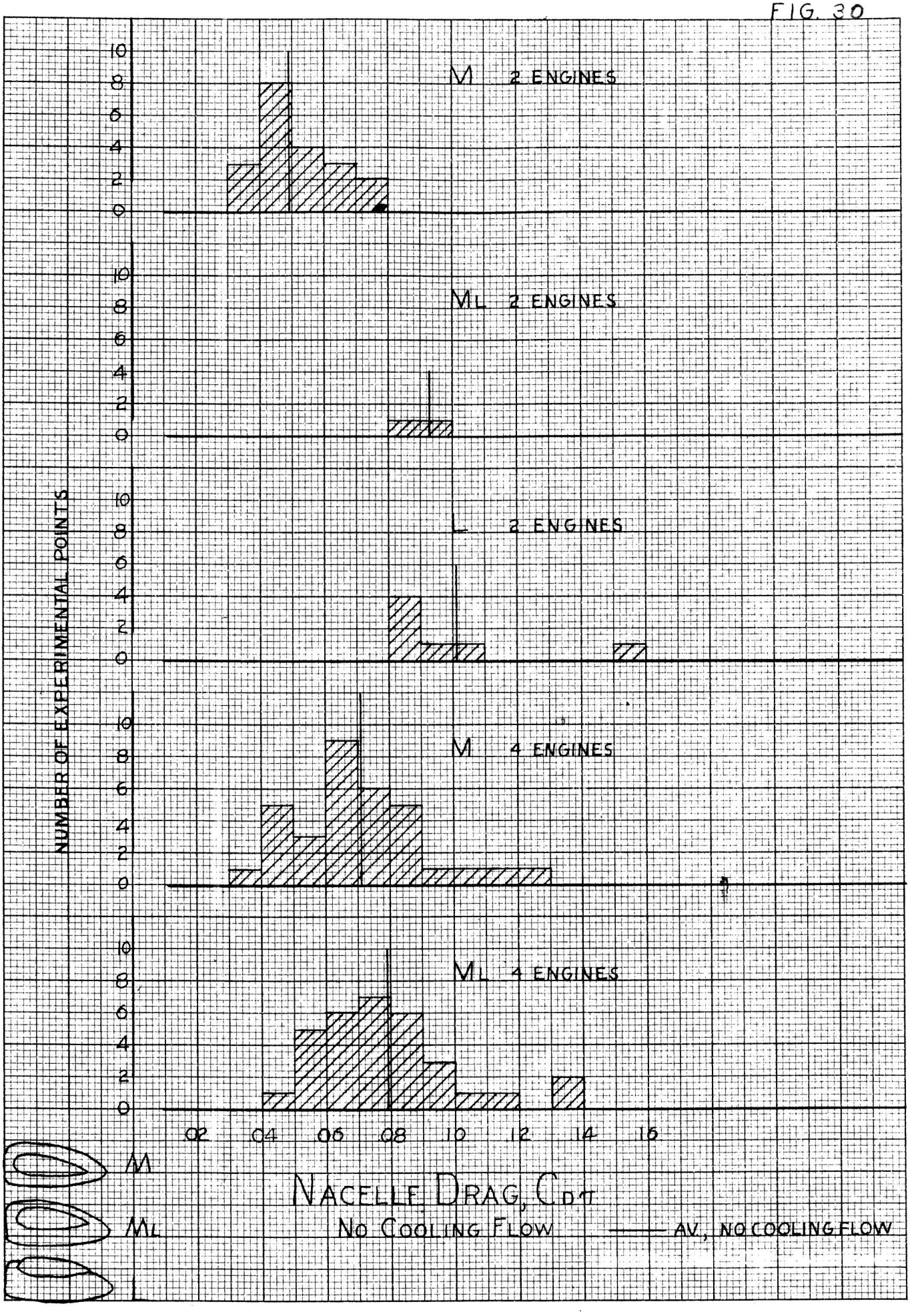
M 2 ENGINES
ML 2 ENGINES
L 2 ENGINES
M 4 ENGINES
ML 4 ENGINES
NUMBER OF EXPERIMENTAL POINTS
0 2 4 6 8 10
02 04 06 08 10 12 14 16
M
ML
NACELLE DRAG, C_{D_T}
NO COOLING FLOW
AV., NO COOLING FLOW

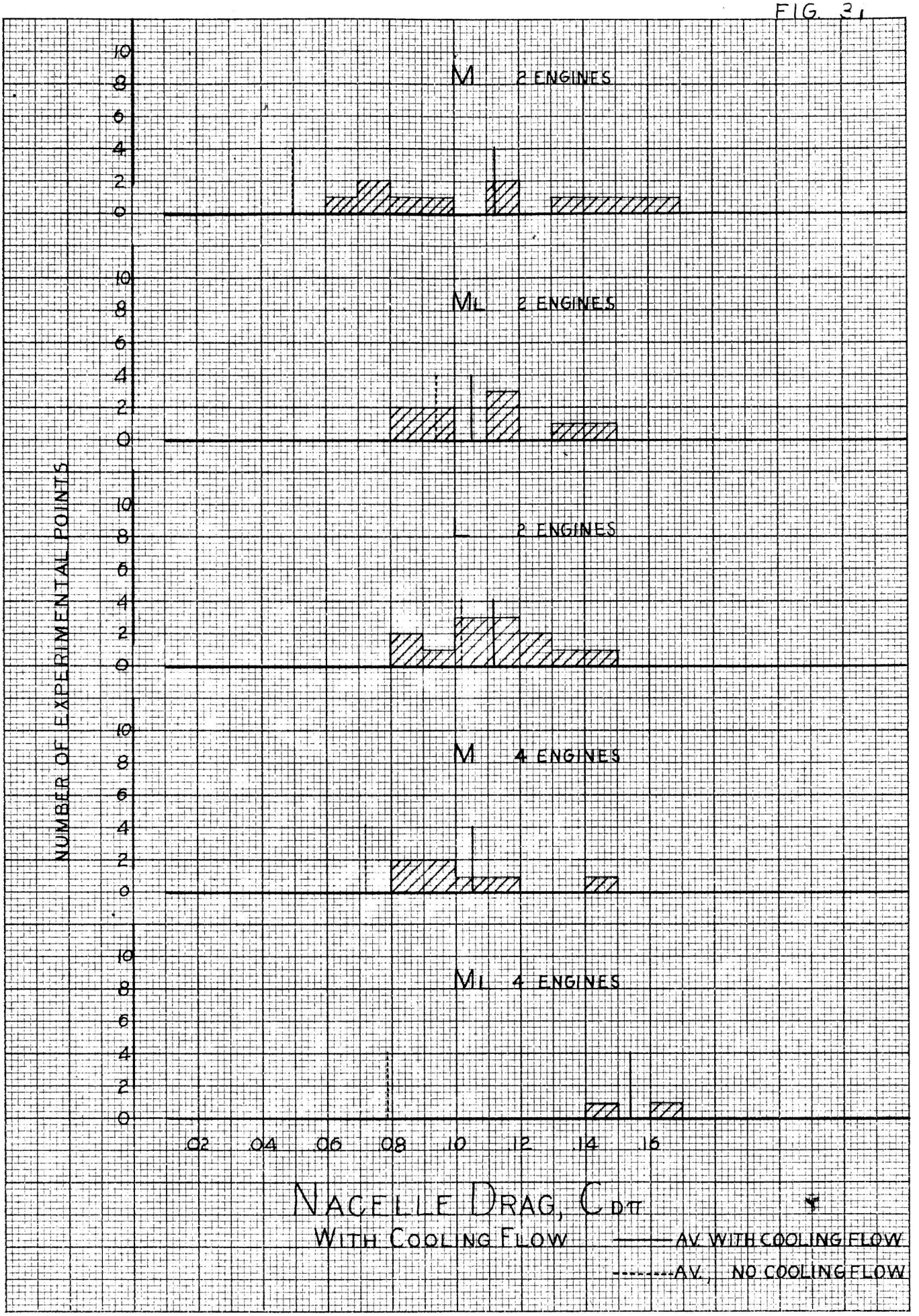
M 2 ENGINES
ML 2 ENGINES
L 2 ENGINES
M 4 ENGINES
ML 4 ENGINES
NUMBER OF EXPERIMENTAL POINTS
0
2
4
6
8
10
.02
.04
.06
.08
.10
.12
.14
.16
NACELLE DRAG, CDπ
WITH COOLING FLOW
AV. WITH COOLING FLOW
AV., NO COOLING FLOW

DESTABILIZING EFFECT OF NACELLES

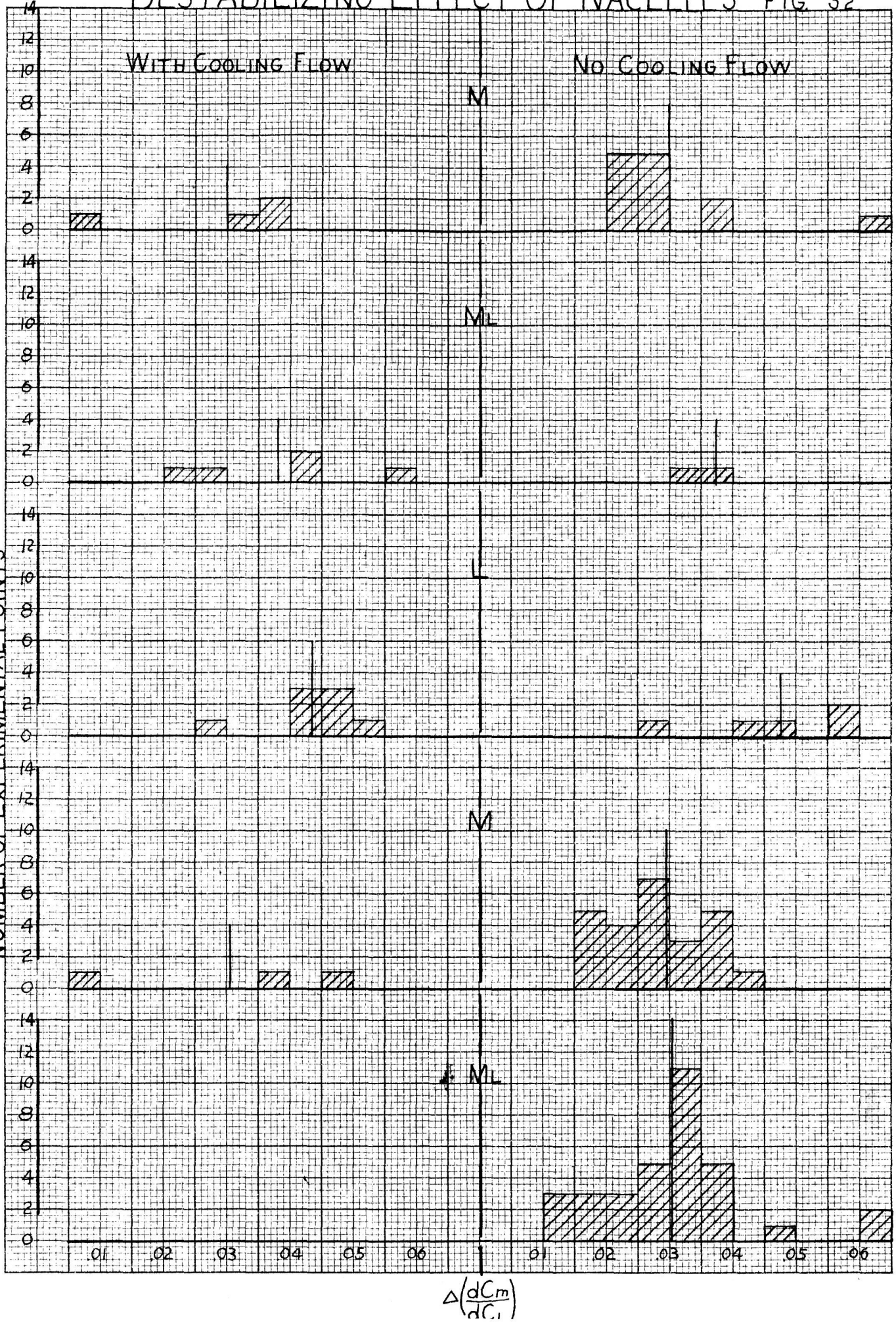

EFFECT OF NACELLES ON C_{M_o}

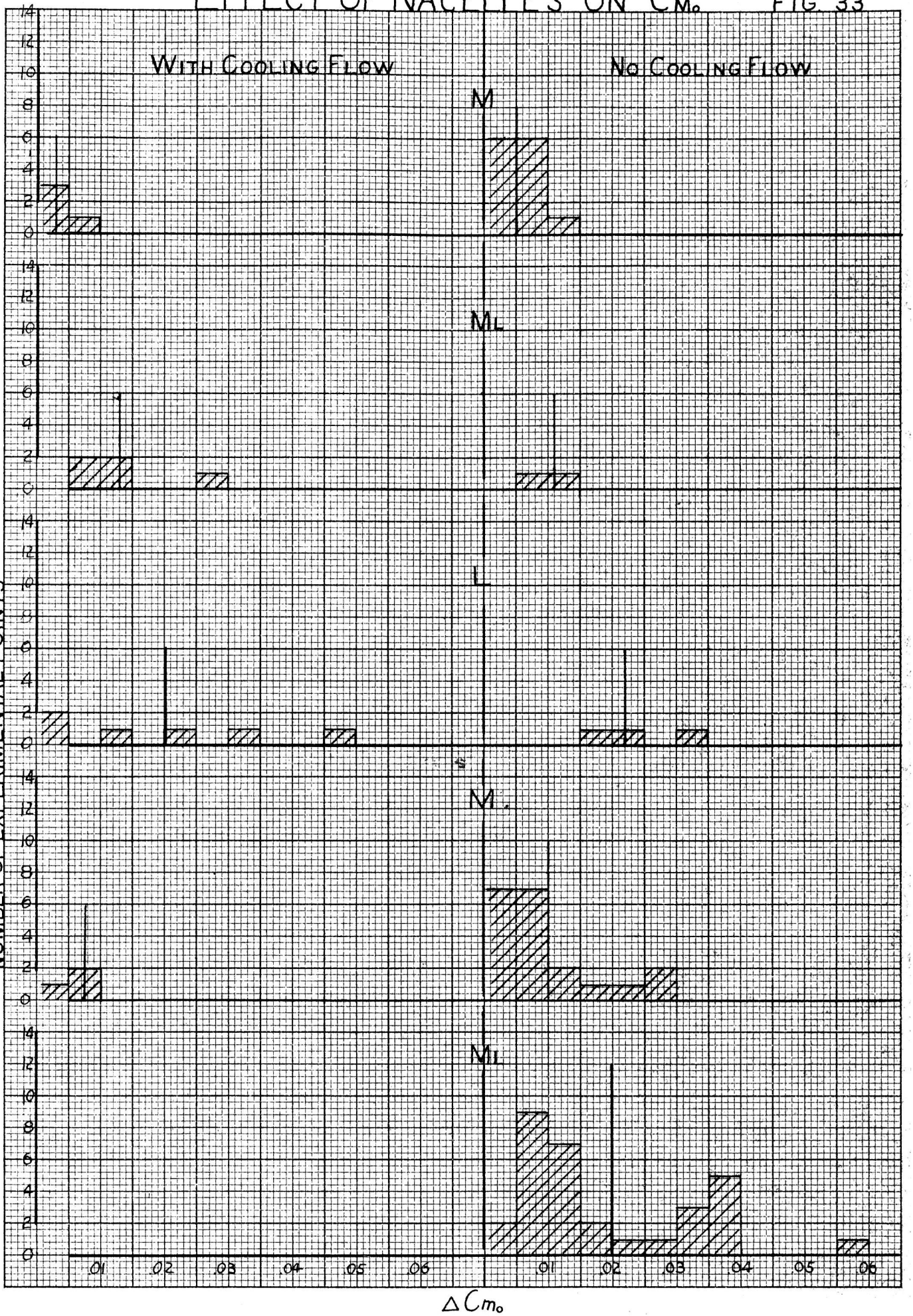

Table II

Notation Used in Following Tables and not Previously Defined

$i \equiv$ incidence of wing

$\alpha_{o_L} \equiv$ angle of attack for zero lift, wing alone

$\frac{h}{r} \equiv \frac{\text{vertical position of } \frac{1}{4} \text{ root chord above center of fuselage cross-section}}{\frac{1}{2} \text{ cross-section height}}$

$\frac{d}{L} \equiv \frac{\text{distance from fuselage nose to } \frac{1}{4} \text{ root chord}}{\text{fuselage length}}$

$\frac{l}{c} \equiv \frac{\text{length of fuselage ahead of } \frac{1}{4} \text{ root chord}}{\text{root chord}}$

C $\backsim$ circular fuselage

S $\backsim$ square-round fuselage

H $\equiv$ maximum height of hull cross-section

w $\equiv$ maximum width of fuselage or hull cross-section

$\frac{y_{c.g.}}{r} \equiv \frac{\text{vertical position of c.g. above middle of fuselage cross-section}}{\frac{1}{2} \text{ cross-section height}}$

C at nac. $\equiv$ wing chord at nacelle center line

$C_{m_{F_1}}$ (for nacelles) $\equiv \frac{M}{q\, S_w (C \text{ at nac.})}$

$C_{m_{F_2}}$ (for nacelles) $\equiv \frac{M}{q\, D\, (C \text{ at nac.})^2}$

D $\equiv$ maximum width of nacelle

i (for nacelles) $\equiv$ angle between thrust line for nacelle and wing reference line

M, M_L, L indicate vertical position of nacelle with respect to wing Cf. fig. 30 for sketches.

H, M, L $\backsim$ high, mid, and low, respectively and are used to indicate vertical position of wing or c.g. with respect to fuselage.

$C_{L_{max.}} \equiv$ increment in maximum lift caused by adding nacelles

c $\equiv$ root chord

M.A.C. $\equiv$ mean aerodynamic chord

$$\frac{n}{c} \equiv \frac{\text{length of hull ahead of leading edge of wing}}{\text{root chord}} \quad \text{(for flying boats)}$$

$$\frac{n}{c} \equiv \frac{\text{length of nacelle ahead of leading edge of wing}}{\text{wing chord at nacelle center-line}} \quad \text{(for nacelles)}$$

Note: All data in the following tables are full scale except the Reynolds Number which is the actual Reynolds Number of the model in the wind tunnel uncorrected for turbulence.

Since true Reynolds Number runs were not made for most of the cases considered here, the Reynolds Numbers given are based on average values of kinematic viscosity for the GALCIT 10-foot tunnel and are, therefore, only approximate.

Possible Errata

Because the tremendous amount of data considered here were collected during a rather short period of time, the author has not been able to check all data, computations, and curves carefully. It is to be expected, therefore, that there are errors in this report. Because of the statistical nature of the work, however, the errors should merely add to the scatter and should not affect appreciably the average values and curves.

TABLE III: MULTI-ENGINE FUSELAGES

F.R.	C_{D_m}	C_L	ΔC_{D_p}	S_w ft.²	S_e ft.²	C_{D_1}	S_f ft.²	L ft.	q lbs/ft.²	R.N.×10⁻⁶	No. Engines	$\frac{h}{r}$	$\frac{d}{L}$	c	Type	Cockpit	i°	$\alpha_{o_L}^\circ$	i_w°	$C_{L_{\alpha_o}}$	$\Delta \frac{dC_m}{dC_L}$	L.A.C. ft.	$\frac{w}{L}$	$\frac{x_{c.g.}}{L}$	$\frac{y_{c.g.}}{r}$	η^*	$\frac{10 C_{m_{f_2}}}{d\alpha_{(rad)}}$	$\frac{10 C_{m_f}}{d\alpha_{(rad)}}$	$\frac{l}{c}$	$i_w C_{L_{\alpha_o}}$	$\Delta C_{D_{f_w}}$	GALCIT Report No.	Fuselage Notations	Remarks
12.94	.132	.30	.0034	4772	4880	.0033	122.8	163	35	8.81	6	.278	.376	33.33'	O	Yes	2½	1.9'	4½	.021	.034	23.39' / 120.1	12.5'	.424	.219	.81	.0613	.990	2.621	.0150	.CZ47	344		XB-36
8.08	.102	.20	.0058	675.9	1055	.0037	38.5	54.5	35	7.66	2	.238	.392	161.3"	C	Yes	3	3.8	6.8	.026	.058	--	6.74'	.395	.000	.86	.1057	1.009	2.135	.0372	.0123	303		NA-63 Revised
9.79	.094	.35	.0039	171 4	2243	.0030	70.58	93	34.2	8.70	4	-.180	.016	204"	O	No	4	1.6	5.6	.033	.049	154.4"	9.5'	.365	.285	.81	.0672	.836	2.281	.0244	.0198	298	B	XB-36 Wing Plan Form similar to
"	.119	.35	.0049	"	"	.0037	"	"	"	"	4	"	"	"	C	"	4	2.4	6.4	.037	.052	"	9.5	.365	.285	.79	.0696	.866	"	.0289	.0194	291	B	Wing of 298 WITH FLAT BRACKETS
8.11	.114	.35	.0057	1422	1928	.0042	70.9	77	35	6.78	4	.50	.361	16'	C	Yes	3	2.0	5.0	.032	.038	138.6"	9.5'	.371	.458	.86	.0599	.615	2.405	.0179	.0133	287	B	XB-32
8.19	.087	.35	.0062	"	2430	.0036	100.9	92.4	35	8.14	4	.580	.374	"	"	"	3	2	5	.044		"	11.34'	.379	.549	.86	.0600	.730	2.992	.0382	.0155	"	B_2	"
8.38	.100	.30	.0050	"	2011	.0035	70.8	79.5	"	7.00	"	.495	.401	"	"	"	"	"	"	.034		"	9.5'	.396	.456	"	.0783	.835	2.76	.0249	.0198	287-F	B	"
8.46	.088	"	.0044	"	1937	.0032	70.9	78.5	"	6.92	"	"	.385	"	"	"	"	"	"	.035		"	"	.381	.456	"	.0801	.845	2.616	.0249	.0206	"	B_1	"
8.74	.106	"	.0053	"	2134	.0035	"	83.0	AVE. 32.5	7.04	"	.483	.384	"	"	No	"	"	"			"	"	.385								282-G	B_2	"
"	.116	"	.0058	"	2115	.0039	"	"	"	"	"	"	"	"	"	Yes	"	"	"			"	"	"								"	$B_{3_{o1}}$	"
"	.114	"	.0057	"	2119	.0038	"	"	"	"	"	"	"	"	"	"	"	"	"			"	"	"									$B_{4_{o1}}$	"
"	.114	"	.0057	"	2117	.0038	"	"	"	"	"	"	"	"	"	"	"	"	"			"	"	"									$B_{4_{c.g.}}$	"
"	.116	"	.0058	"	"	.0039	"	"	"	"	"	"	"	"	"	"	"	"	"			"	"	"									B4	"
"	.114	"	.0057	"	"	.0038	"	"	"	"	"	"	"	"	"	"	"	"	"			"	"	"									B	"
"	.116	"	.0058	"	2119	.0039	"	"	"	"	"	"	"	"	"	"	"	"	"			"	"	"									B4 C	"
8.67	.104	"	.0052	"	2040	.0036	"	82.35	"	6.98	"	"	.379	"	"	No	"	"	"			"	"	.380									B5	"
"	.104	"	.0052	"	2025	.0037	"	"	"	"	"	"	.379	"	"	Yes	"	"	"			"	"	"									B	"
7.04	.111	0.4	.0073	1048	-	-	6.88	65.95	35	7.74	"	.428	.358	14'	S	Yes	3	1½	4.2	.029	.045	123.6"	7.46'	.366	.266	.84	.0790	.564	2.240'	.0174	.0164	285		Consolidated Model 32
6.72	.110	.20	.0072	"	1572	.0048	"	62.95	"	7.38	"	.513	.330	14'	S	"	"	2	5	.029	.033	123.5"	"	"	.268	.83	.0628	.427	2.018	.0112	.0145	279	B	" LB-30
6.78	.109	"	.0071	"	1525	.0047	"	63.4	"	7.44	"	"	.364	14'	S	"	"	"	"	-	-	"	"	.340	"	"	-	-	-	-	-	-	B_1	" "
7.85	.100	"	.0057	673.8	1011	.0038	38.5	54.96	"	7.75	2	.238	.392	161.13"	C	"	"	4	7	.032	.060	140.1"	7.00'	.378	.155	.73	.0879	.878	2.151	.0366	.0146	277	B	NA-63
8.38	.115	"	.0075	146 3	2600	.0042	95.49	92.25	"	8.40	4	-.729	.349	215.51"	C	"	4	5.2	9.2	.040	.070	165.6"	10.52	.354	-.354	.76	.0715	.759	2.360	.0537	.0099	271	B	DC-4
8.74	.116	"	.0057	464.8	730?	.0036	22.7	47.2	"	7.38	2	.171	.348	132.35"	S	"	3	3.7	6.7	.020	.030	100.2"	4.12	.348	.514	.71	.0723	.613	1.968	.0200	.0107	263		A-20-A (S_5 Down
8.29	.108	"	.0054	126 7	1750	.0039	63.6	74.75	"	7.54	4	.514	.369	15.30'	C	"	3	3.8	6.8	.020	.036	133.6"	9.00	.333	.482	.85	.0534	.563	2.291	.0227	.0087	258	B	LB-25
8.66	.93	.2	.0048	609.35	879	.0033	31.4	54.72'	"	8.56	2	.040	.369	154"	S	"	"	1.1	4.1	-	-	116.33"	4.7	.358	.061	.72	—	-	-			253-R	B	NA-62
"	"	"	"	"	890	.0033	"	"	"	"	"	"	"	"	S	"	"	1.1	4.1	.025	.041	"	"	.358	"	"	.0779	.640	2.083	.0133	.0210	"	B_d	"
8.47	.113	"	.0060	"	879	.0042	"	53.5	"	8.37	"	"	"	"	S	"	"	1	4	.022	.029	"	"	.344	-.05	"	.0575	.463	2.028	.0092	.0194	253-A	B	"

TABLE II (CON'T.)

F.R.	C_{D_m}	C_L	ΔC_{D_p}	S_w ft²	S_s ft²	C_{D_s}	S_r ft²	L ft.	q gm/cm²	R.N.×10⁻⁶	No. Engines	$\frac{h}{r}$	$\frac{d}{L}$	C	Type	Cockpit	i°	α_o°	i_w°	ΔC_{m_o}	$\Delta\left(\frac{dC_m}{dC_L}\right)$	M.A.C.	W	$\frac{X_{cg.}}{L}$	$\frac{Y_{c.g.}}{r}$	η *	$\frac{dC_{m_F}}{d\alpha_{(rad)}}$	$\frac{dC_{m_F}}{d(\alpha_{rad})}$	$\frac{l}{c}$	$i_w^\circ \frac{d\alpha_t}{di_w}$	$\Delta C_{m_{F_t}}$	GALCIT Report No.	Fuselage Notation	Remarks
6.55	.080	.30	.0060	1267	1968	.0039	95.03	71.1'	35	7.38	4	.625	.354	15.2'	C	No	2.8	2.1	4.9	.040	.049	132.6	11.0	.361	.380	.84	.0615	.520	2.340	.0221	.0164	249	B	LG-4 (Wing locaton is only change)
8.40	.123	"	.0069	"	2178	.0040	70.83	84.0	35	8.46	"	.572	.413	"	C	Yes	2.7	"	4.8	.050	.090	"	9.5	.427	.189	"	.0990	1.118	3.133	.0398	.0245	"	B_S	
"	.127	"	.0071	"	2178	.0041	70.83	84.0	"	8.46	"	.716	"	"	"	"	2.8	"	4.9	.053	.074	"	"	"	.272	"	.0815	.919	3.139	.0334	.0245	"	B_S'	
5.83	.78	"	.0073	"	2038	.0045	119.36	71.8	"	7.22	"	.183	.321	"	S	No	3.2	"	5.3	.037	.047	"	"	.358	.286	"	.0705	.406	2.083	.0230	.0114	"	B_d	Change in Aft Portion
5.56	.79	"	.0074	"	2162	.0043	"	68.4	"	6.88	"	"	.337	"	S	"	"	"	"	.041	.048	"	"	.343	"	"	.0798	.436	2.087	.0235	.0133	"	B_d'	
6.81	.85	.20	.0056	1048	1503	.0039	68.8	63.7	"	7.47	"	.293	.323	14.0'	S	Yes	3	2.8	5	.033	.028	123.66	7.46	.334	.265	.82	.0614	.356	1.996	.0126	.0163	243		B-24
6.19	.95	"	.0074	1000	1788	.0041	77.9	61.6	"	8.66	"	.774	.343	14.83'	ELLIPSE	Yes	"	4.4	7.4	.047	.047	139	8.616	.355	.720	.76	.0793	.540	1.825	.0286	.0153	242		
8.78	.87	.2	.0039	550	749	.0029	24.6	49.2	"	10.84	2	.504	.335	153"	ELLIPSE	No	2	3.9	5.9	.030	.020	114.1'	4.72	.304	.621	.74	.0594	-	-	-	-	238	B_1	
"	.83	"	.0037	"	"	.0027	"	"	"	"	"	"	"	"	S	"	2	-	-	-	-	"	"	"	"	"	"	-	-	-	-	-		B_1X_1	
10.48	.120	"	.0033	5985	638	.0031	16.42	47.97	"	7.50	"	-.023	.335	154"	S	Yes	3	3.8	6.8	.005	.015	116.2'	3.19	.329	-.248	.72	.0540	.504	1.659	.0081	.0054	237		
8.65	.125	"	.0050	"	788	.0038	24.0	47.8	"	7.48	"	-.598	.372	"	S	No	3	4.0	7.0	.010	.020	"	3.785	.361	.408	"	.0607	.467	1.835	.0111	-	236	B	
8.55	.122	.20	.0049	598.5	774	.0038	24.0	47.3	"	7.40	2	.598	.365	154"	S	No	3	4	7	-	.020	116.2'	3.785	.354	.408	.72	.0619	.462	1.780	.0111	-	236	B_2	
9.09	.115	"	.0046	"	818	.0034	"	50.3	"	7.88	2	"	.405	"	S	No	3	4	7	—	—	"	"	-	"	"						"	B_3	
6.99	.079	.2	.0050	1048	1498	.0035	66.1	64.2	"	7.45	4	.341	.321	14'	S	No	"	1.8	4.8	.032	.035	123.5'	7.25	.33	.290	.85	-	.295	2.001	.0156	.0170	234-A	B_{1_F}	Model 32
"	.076	.2	.0048	1048	"	.0034	66.1	"	"	"	4	"	"	"	S	No	"	"	"	-	-	"	"	-	"	"	-	-	-	-	-	"	B_1	B_1 with FAIRING
8.18	.095	.3	.0047	2155	2572	.0039	106.6	94.75	"	8.01	4	-.566	.307	25.1'	S	Yes	3.75	4.7	8.45	.033	.028	212.[illegible]	9.96	.356	-.041	.75	.0563	.499	1.643	.0195	.0148	212		
7.68	.094	.2	.0069	1200.8	2067	.0040	85.2	80.0	"	7.51	2	-.67	.424	17.83'	C	No	3	1.8	4.8	.045	.072	12.80	10.59	.433	-.238	.76	.0775	.778	2.65	.0515	.0212	225	B_5X_1	
"	.100	"	.0073	"	"	.0042	"	"	"	7.51	2	"	"	"	C	No	0	"	1.8	.020	.090	"	"	.433	-.238	.76	.0971	.975	2.65	.0135	.0252	225-A	"		

Additional Multi-engine Fuselage Data not including C_{D_s}

F.R.	$C_{D_{fl}}$	C_L	ΔC_{D_p}	S_w ft.^{2}	S_{fl} ft.^{2}	L ft.	q gm/cm^2	R.N.$\times 10^{-6}$	No Engines	Vertical Wing Position	Type	Cockpit	i°	$\alpha_{o_L}{}^\circ$	$i_w{}^\circ$	ΔC_{m_o}	$\Delta \frac{dC_m}{dC_L}$	M.A.C.	$\frac{X_{c.g.}}{L}$	$\frac{y_{c.g.}}{L}$	η_{tv}	$\frac{d\sigma_{m_{FS}}}{d\alpha_{(rad)}}$	$i_w \frac{dC_m}{di_w}$	$\frac{\Delta C_{m_{FS}}}{i_w}$	SALSIT Report No.	Fuselage Notation	Remarks
6.71	.098	.2	62	800	50.8	54	35	7.64	3	L	C	Yes	3	4	7	.042	.055	10'	.38	L	74	.735	.0312	.0175	240	$P_{N_{1c}}X$	Ranger } Transair
"	.104	"	66	"	"	"	"	"	3	L	"	Yes	"	"	"	.034	.041	"	"	L	"	.555	.0232	.0142		$IN_{2c}X$	Radial }
7.05	.125	"	72	1048	60.4	61.8	"	7.42	4	H	DC	Yes	"	1.8	4.8	.016	.023	10.27	.35	.22	84	.351	.0101	.0060	234	B	
6.92	.090	"	68	1201.5	90.7	74.4	"	7.47	2	L	C	No	0	1	1	.015	.055	160.8"	.449	-.233	74	1.220	.0055	.0250	229	B_6X,	
7.52	.129	.3	70	1048	57.0	64.0	"	7.98	3	H	DC	Yes	3	1.8	4.8	.010	.030	10.27	.38	.32	85	.472	.0135	.0062	224	BX	Consolidated
				Same with Aft fairing							C					.020	.035	"	"	"	"	.554	-				
4.96	.070	.4	52	1353	101	56.25	35	4.95	2	L	S	No	3.5	1.2	4.7	.040	.042	13.69'	.373	L	73	.627	.0501	.0277	203	BX,	CW-20
6.62	.075	.2	60	551	44.4	49.8	35?	9.34	2	L	S	Yes	-	0.8	-	.029	.016	115.8	-	L	75	-	-	-	187		Lockheed 14
5.85	.068	.3	55	551	"	44.0	"	8.26	2	L	S	"	2	-	-	-	-	"	-	-	-	-	-	-	177	B,T	Lockheed S-10
7.66	.104	.2	59	2155	122.3	95.61	"	7.48	4	L	C	"	3.75	5	8.75	.028	.035	17.70	.36	M_L	77	.547	.0256	.0104	175		DC-4
8.19	.086	.2	46	402	21.6	43	"	7.56	2	H	S-E	"	3	4.4	7.4	.016	.019	99.8	.325	H	73	.296	.0093	.0078	174	BDX	N.A. 7-A Observation
6.41	.072	.26	51	471	34.83	42.68	"	8.01	2	L	S	"	2	5.1	7.1	.028	.027	11 0"	.34	L	71	.320	.0150	.0114	173		Lockheed S-10
7.05	.119	.26	64	1120	60.1	61.6	"	7.22	2	M	S	Yes	2.5	1.6	4.1	-		154.7	.28	M	74	-	-	-	171		N.A.-21
-	.082	-	44	987	52.9	-	"	-	2	-	C	Yes	-	3.5	-	-		-	-	-	73	-	-	-	164		DS-T
9.46	.104	-	38	1946	70.8	89.8	"	8.43	4	L	C	No	1.6	3.6	5.2	.012	.028	238.4	.367	-.512	74	.690	.0118	.0123	152		CW P 212
8.65	.087	-	46	910	48.2	67.8	35?	8.68	2	L	S	Yes	2	1.7	3.7	.013	.006	11.7	-	M	74	.091	.0183	.0115	149		DB-1
-	.073	-	40	987	52.9	-	35	-	2	-	C	Yes	-	3.5	-	-	-	-	-	-	73	-	-	-	147		DC-3
10.11	.078	-	26	1420	47.5	78.67	40?	6.58	4	M		Yes	3.6	3.2	6.7	.014	.026	177.1	.304	M	84	.636	.0132	.0118	145		Boeing 299
	.059	-	36	"	86.5		"	"	"																		" 300 (square)
	.069	-	42	"	86.6		"	"	"																		" 300 (round)
	.093	-	44		44.4																						
	.076	-	55		20.5																						

TABLE IV: SINGLE ENGINE FUSELAGES

C_L	$C_{D_{fp}}$	ΔC_{D_p}	S_w (ft^2)	S_{fp} (ft^2)	L ft.	q gm/cm^2	R.N. $\times 10^{-6}$	HML wing	F.R.	i°	$\alpha_{o_L}^\circ$	i_w°	ΔC_{m_o}	$\Delta\left(\frac{dC_m}{dC_L}\right)$	M.A.C	$\frac{X_{c.g.}}{L}$	HML c.g.	Cooling flow	$\frac{dC_{m_{fp}}}{d\alpha}$ (rad)	$i_w\frac{dC_m}{d\alpha}$	Fuselage Notation	GALCIT Rep.	Remarks
.15	.091	.0063	375	26.0	38.31	35	10.11	Gull wing at M	6.80	2	3.8	5.8			1044"	.32	M	.70	No			$B\text{-}T_uT_Lt_s$	323	Douglas 230 Dive Bomber
.15	.107	.0074	"	"	"	"	"		"	2	"	"	.024	.043	"	.32	M	"	"	.624	.0192	B		
--	.084	.0061	183.5	13.0	29.6	25	8.70	L	7.27									.62				B_ND	321	CW XP-55
.21	.095	.0066	332	23.06	36	35	8.45	L	6.74				.006	.024	91.1"	.264	-2	.62	"	.236			289	Vultee Dive Bomber
.15	.109	.0057	233.4	12.2	31.25	15	7.20	L	7.93	1	2	3	.017	.034	79.6"	.33	L	.70	"	.608	.0079	B_s	286	
"	.113	.0059	"	"	"	"	"	L	"	1	2	3		.036	"	.33	L	"	"	.647	.0083	B_{ls}		
.2	.098	.0073	330	24.52	36.5	35	8.57	H	5.53	4	5.5	9.5	.018	.024	80.25"	.26	H	"	"	.261	.0176	$BCK_l'L_r$	254	DS 293
"	.101	.0075	"	"	"	"	"	H	"	4	"	"			"	"	H	"	"			BCK_lL_r		Different Cockpit enclosures
"	.106	.0074	"	22.96	"	"	"	H	6.76	4	"	"			"	"	H	"	"			BCK_2L_r		
"	.102	.0067	442	20.15	3[illegible].45	"	8.22	M	6.41	2	"	"				".28	.00					BC	232	Svenska L-10
.16	.104	.0069	199.7	15.0	27	30	8.45	L	6.18						69.07								231	Vultee XP 48
.2	.107	.0088	232.2	19.1	-	"	-	L								.28	L	.84					231-A	" XIC-51
"	.098	.0060	156.5	9.57	22.5	35	7.92	L	6.45		1.2		.011	.023	61.50"	.28	L	.69	"	.374		BK	210	Lobil Basic Trainer
.3	.094	.0094	294	29.2	29.8	"	8.38	L	4.89	3	1.6	4.6	.030	.023	91.22"	.27	L	.65	"	.242	.0248		208	Airover
"	.094	.0093	"	"															Yes			B_{3N}	208-A	"
"	.075	.0074	"	"																			"	"
.25	.145	.0069	218	10.4	27			L	5.82	2	3.8	5.8	.006	.026	6.195'	.27	M_L	.69	Yes	.545	.0115	$B_2C_2K_2X_3$	180	NATIONAL (BASIC TRAINER)
"	.093	.0079	352	29.6	37.67	35	7.56	L	6.14	2	2.8	4.8			93.7"			.72	No				158	LOCKHEED 11
	.126	.0050	315	12.5	2917			L	7.44		4.2	4.2	.003	.008	17.5"	.25	L	.66	"	.226	.0023		141	Northrup XBT-1
	.124	.0063	420	21.3	33.92	35	7.35	L	6.51		4.7	4.7	.004	.008	109.3"	.28	L	.81		.217	.0034		136	XTBD-1
	.077	.0052	384	26.1	37	"	7.43	L	6.42	0	5.7	5.7	.017	.03	100.5"	.323	M	.69	Yes	.535	.0142		125	ADC-Vultee
	.049	.0028	-	10.1																			140	NORTHRUP XFT-1
	.107	.0072	172	11.55	23.17			H	6.04	1.9	2.2	4.1	.040	.080	6.51'	.25	M	.69	Yes	1.220	.0250		115	Boeing 253
	.117	.0080	169.5	11.60	24.75			L	6.48	1	2.3	3.3	.012	.059	74.8"	.223	M	.65	"	.885	.0139		112	Boeing 255
	.094	.0056	363	21.7	30.7	45	7.4	L	5.84	2,5	3.1	5.6	.008	.012			L	.76	No				110	Northrup 1A
	.066	.0020	"	11.05	28.9	"	6.96	L	7.70	"	"	"	.002	.003			L	.85	"				"	" 2A

TABLE V : FLYING BOAT HULLS

C_L	$C_{D_{fp}}$	ΔC_{D_p}	S_w (ft^2)	S_{f_p} ft^2	L ft.	q gm/cm^2	R.N.$\times 10^{-6}$	No. Engines	Cockpit	i	$-\alpha_{O_L}$	i_w	ΔC_{m_o}	$\Delta\left(\frac{dCm}{dC_L}\right)$	M.A.C.	$\frac{X_{c.g.}}{L}$	H M L (Vertical Wing Position)	η_{tx}	$\frac{dCm_f}{d\alpha_{(rad.)}}$	$i_w^\circ \frac{dCm}{d\alpha^\circ}$	H (Max. Ht.)	W Max. Width	$\frac{w}{c}$	F.R.	$\frac{\Delta C_{M_F}}{i_w}$	Hull Notation	GALCIT Report No.	Remarks
.20	.122	.0111	1823	165.9	94.40	34.18	8.79	2	Yes	4°	1.6°	5.6°	.048	.053	165.2"	.36	H	.77	.415	.0248	17.4'	10.35'	1.78	6.5	.0123		297	BOEING XPBB-1
.20	.117	.0106	"	165.9	92.98	"	"	"	"	"	"	"	WITH TURRETS .040		"	.35	"	"				10.35'	1.675	6.4	-	B_1	290	WITH TURRETS " "
"	.118	.0107	"	"	"	"	"	"	"	"	"	"	.043		"	.35	"	"	.382	.0191	17.4'	"	"	6.4	-	B_2		SAME HULL
"	.114	.0104	"	"	"	"	"	"	"	"	"	"			"	.35	"	"	.411	.0205	"			"		B_3		WITH VARIOUS FAIRINGS
"	.120	.0109	"	"	"	"	"	"	"	"	"	"			"		"	"						"		B_4		
"	.121	.0110	"	"	"	"	"	"	"	"	"	"			"		"	"						"		B_5		
"	.123	.0112	"	"	"	"	"	"	"	"	"	"			"		"	"						"		B_6		
"	.112	.0102	"	"	"	"	"	"	"	"	"	"			"		"	"						"		B_7		
"	.112	.0102	"	"	"	"	"	"	"	"	"	"			"		"	"						"		B_8		
"	.112	.0102	"	"	"	"	"	"	"	"	"	"			"		"	"						"		B_9		
"	.112	.0102	"	"	"	"	"	"	"	"	"	"			"		"	"						"		B_{10}		
.45	.091	.0110	1267	153.5	80.17	35	8.06	2	Yes	3°	+2°	5°	.060	.256	11.05'	.361	H	.84	.336	.0258	16.2'	10.0'	1.570	5.73	.0137		257	CONSAIR BM-7
"	.087	.0105	"	"	"	"	"	"	"	"	"	"	.062	.061	"	"	H	"	.366	.0280	16.2'	10.0'	"	"	.0141	B_1	257-A	
.4	.079	.0097	1048	129.0	69.6	35	8.24	2	"	"	"	"	.060	.058	10.30'	.342	"	.82	.360	.0269	15.5'	8.33'	1.41	5.44	.0144	B	251	CONSAIR MODEL 31
"	.084	.0104	"	"	"	"	"	2	Yes	"	"	"	.071	.054	"	"	"	"	.335	.0243	"	"	"	"	.0171	B_1	"	← (BEAVER TAILED PLANING SURFACE.
.5	.075	.0092	1048	129	69.6	"	"	2	Yes	"	"	"	.060	.062	10.27'	.342	"	.84	.392	.0286	15.5'	"	"	"	.0144		222	CONSAIR 31
.5	.102	.0068	1780	118	77.1	35	7.75	4	Yes	"	+6.5°	4.6°	.014	.012	193.5"	.30		.73	.192	.0044	13.28'	10.5'	0.8 65	6.29	.0096	B_1	221	XPB2Y-1
"	.112	.0074	"	"	"	"	"	"	"	"	"	"	-	-	"	-	-	"	-					"		B		
"	.100	.0074	"	130	78.3	"	7.8 8	"	"	"	"	"	-	-	"	-	-	"	-					6.09		B_2		
.5*	.091	.0106	1000	116	66.25	35	7.9	2	No	2.0	1.9°	4.5°	.050	.027	10.53'	.365	H	.81	.201	.0109	15.5'	8.33'	1.23	5.13	.0162	B	218	CONSAIR MODEL X
.5**	.090	.0104	"	"	66.5	"	"	"	"	2.6°	"	4.8°	.042	.042	"	.324	H	"	.292	.0179	"	"	"	5.46	.0119	B_3		
	.130	.0076	1296	77.6	66.16	"	7.88	"	Yes	-	+6.8°	6.8°	.022	.027	175.1'	.36	H	.68	.435	.0177	10.8'	8.33'	1.1	6.74	.0123		127 129 137	DOUGLAS XPBD-1
	.156	.0107		75.6																								" YOA-5

* i = 2.6 FOR DRAG.

** i = 2.9 " "

TABLE VI : NACELLES

(All dimensions full scale)

C_L	C_{D_n}	ΔC_{D_p}	S_n ft.²	S_w ft.²	M.A.C.	C at Nac.	D	M M_L L	No. Engines	$\Delta C_{L_{MAX}}$	$-\Delta C_{m_o}$	$\Delta\left(\frac{dC_m}{dC_L}\right)$	i	α_{0_L}	iw	η_*	$\frac{\eta}{c}$	Cooling Flow	$\frac{dC_{nF2}}{d\alpha_{rad}}$	$\frac{dC_{nF1}}{d\alpha_{rad}}$	GALCIT Report No.	Nacelle Notation	Remarks
.4	.059	.0019	33.8	1048	10.30'	12.2'	5.04'	M_L	4	-.03	.025	.035	30°	-2°	5°	.85	.520	No	2.69	4.89	326	NI_1	X-24
.4	.071	.0023	"	"	"	9.9'	"	"	"	.01	.017	.033	"	"	"	"	.714	"	3.34	5.69	"	N_{O_1}	"
.4	.062	.0020	"	"	"	12.2'	"	"	"	-.07	.033	.034	"	"	"	"	.520	"	2.60	4.70	"	N_{I_2}	"
.4	.087	.0028	"	"	"	9.9'	"	"	"	.01	.010	.033	"	"	"	"	.714	"	3.34	5.69	"	N_{O_2}	"
.4	.055	.0018	"	"	"	12.2'	"	"	"	-.05	.038	.033	"	"	"	"	.520	"	2.54	4.61	"	N_{I_3}	"
.4	.086	.0028	"	"	"	9.9'	"	"	"	-.01	.012	.033	"	"	"	"	.714	"	3.34	5.69	"	N_{O_3}	"
.25	.104	.0067	34.95	540.44	97.53"	9.2'	4.72'	L	2	.10	.034	.044	20°	-2.7°	4.7°	assume .85	.727	Cowl Flap Closed	2.60	3.24	318	N	Douglas 990
.35	.065	.0025	66.2	1714	154.41"	15.2'	5.74	M	4	.01	.007	.036	30°	-1.6°	4.6°	.82	.498	No	3.10	3.29	298	N_2	Boeing X B-29
"	.081	.0018	60.4	"	"	12.8'	5.59'	"	"	.02	.004	.018	"	"	"	"	.590	"	2.25	2.66	"	N_4	"
"	.060	.0022	63.0	"	"	15.2'	5.61'	"	"	.02	.003	.027	"	"	"	"	.497	"	2.38	3.22	"	N_{in}	"
"	.050	.0015	51.0	"	"	12.8'	5.31'	"	"	.01	.006	.022	"	"	"	"	.599	"	2.87	3.84	"	N-Nin	"
"	.067	.0026	66.2	"	"	15.2'	5.74'	"	"	0	-	.038	"	"	"	"	.498	"	3.27	4.33	"	N_5	"
"	.067	.0026	66.2	"	"	"	"	"	"	0	-	.037	"	"	"	"	"	"	3.18	4.20	"	N_6	"
"	.065	.0025	66.2	"	"	"	"	"	"	0	-	.036	"	"	"	"	"	"	3.10	4.10	"	N_7	Boeing X-B-29
.20	.038	.0010	47.6	1823	165.22"	16'	5.51'	"	2	0	.001	.023	-	-1.6°	-	.78	.28	No	2.01	3.67	297	N_3	Boat
.35	.082	.0030	63.0	"	"	-	-	"	4	-	-	-	-	-	-	-	-	"	-	-	291	Nin	Same as 298
.35	.047	.0014	51.0	"	"	-	-	"	4	-	-	-	-	-	-	-	-	"	-	-	-	N-Nin	
.2	.042	.0011	47.6	"	"	-	-	"	2	0	.005	.015	-	-	-	-	-	"	-	-	290	N3	Same as 297
.35	.090	.0036	57.2	1422	11.55'	13.8'	6.11'	M	4	-.06	.033	.011	20°	-2.0°	5°	.86	.524	No	.84	1.23	287	N_I	One of several configurations tested
.35	.087	.0035	57.2	"	"	"	"	"	"	-.10	-	.034	"	"	"	"	"	"	2.57	3.80	"	N_I	"
"	.064	.0026	"	"	"	"	"	"	"	-.08	.057	.032	"	"	"	"	"	"	2.44	3.60	"	N_{I_1}	
"	.131	.0053	"	"	"	11.2"	6.00'	"	"	-.11	.006	.037	"	"	"	"	.658	"	4.44	5.00	"	No	One of several configurations tested (F) denotes rearfaired aft of T.E.
"	.087	.0035	"	"	"	"	"	"	"	-.10	.013	.034	"	"	"	"	"	"	4.07	4.62	"	No	

TABLE VI, Page 2

C_L	C_{D_F}	ΔC_{D_P}	S_F ft²	S_W ft²	M.A.C.	C at Nac.	D	M / M_L	No. Engines	$\Delta C_{L_{MAX.}}$	ΔC_{M_o}	$\Delta\left(\frac{dC_m}{dC_L}\right)$	i	α_{o_L}	i_W	η_H	$\frac{\eta}{C}$	Cooling Flow	$\frac{dC_{m_{F_2}}}{d\alpha_{(rad.)}}$	$\frac{dC_{m_{F_1}}}{d\alpha_{(rad.)}}$	GALCIT Report No.	Nacelle Notation	Remarks
.35	.038	.0023	56.0	1422	11.55'	11.8 '	6.00'	M	4	-.04	-	.06	30	-2.0°	5°	.86	.658	No	7.80	6.40	287	No_1	
"	.117	.0047	57.2	"	"	"	"	M_L	"	-.09	-	"	"	"	"	"	"	"	"	8.93	"	No_2	VARIOUS FAIRINGS OF N_o
"	.092	.0037	57.2	"	"	"	"	M_L	"	-.07	-	"	"	"	"	"	"	"	"	8.93	"	No_3	
0.35	.062	.0023	58.4	"	"	13.8'	5.77'	M_L	"	-.04	.034	.018	"	-2°	"	"	.524	"	1.45	2.20	287-A	N_I	
"	.081	.0030	"	"	"	"	"	"	"	0.08	.028	.013	"	"	"	"	"	"	1.06	1.60		N_{I_2}	
"	.060	.0024	57.2	"	"	"	6.11	"	"	-.05	.040	.047	"	"	"	"	"	"	3.59	5.30		N_{I_3}	
"	.062	.0023	58.4	"	"	13.33	5.89	M	"	-.03	.013	.020	"	"	"	"	"	"	1.69	2.54		N_{I_4}	
"	.069	.0030	62.0	"	"	"	"	M	"	-.05	.018	.018	"	"	"	"	"	"	1.52	1.93		N_{I_7}	
"	.074	.0028	58.6	"	"	"	"	M	"	-.03												N_{I8}	
"	.060	.0024	57.2	"	"	11.3'	6.00'	M_L	"	0	.006	.040	"	"	"	"	.658	"	4.60	5.50		No	
"	.098	.0036	52.4	"	"	11.3'	5.84'	M_L	"	-.04	.011	.053	"	"	"	"	"	"	3.92	4.95		No_1	
"	.109	.0040	"	"	"	"	5.84'	"	"	-.03	.013	.030	"	"	"	"	"	"	3.56	5.39		No_2	
"	.136	.0050	"	"	"	"	"	"	"	-.02	.015	.028	"	"	"	"	"	"	3.34	4.21		No_3	
"	.095	.0035	"	"	"	"	"	"	"	-.07	.010	.020	"	"	"	"	"	"	2.38	3.00		No_4	
"	.075	.0030	57.2	"	"	"	6.00	"	"	-.06	.007	.037	"	"	"	"	.658	"	4.35	5.06		No_5	
"	.065	.0024	52.4	"	"	11.1'	5.89	M	"	-.02	.006	.040	"	"	"	"	.686	"	4.89	6.10		No_6	
"0.3	.078	.0031	56.6	"	"	13.8'	5.92'	M_L	"	-.023	.039	.030	"	"	"	"	.58	"	2.36	3.40	282-F	NI_9	
"	.080	.0039	56.6	"	"	11.1'	"	M	"	-.082	--	.030	"	"	"	"	.74	"	3.65	4.22		No_7	
"	.078	.0031	"	"	"	"	"	M	"	-.090	-	.030	"	"	"	"	"	"	3.65	4.22		No_8	
"	.080	.0032	"	"	"	"	"	"	"	-.090	-	.061	"	"	"	"	"	"	3.77	4.37		No_8	
"	.078	.0031	"	"	"	"	"	"	"	-.107	-	.027	"	"	"	"	"	"	3.28	3.79		No_9	
"	.063	.0021	47.2	"	"	11.1	5.71	M	"	-.05	.010	.025	"	"	"	"	"	"	3.6	3.70	287-G	No_{11}	
"	.075	.0030	56.6	"	"	13.8	6.0	M_L	"	-.05	.040	.017	"	"	"	"	58	"	1.31	1.92		NI_{10}	

TABLE VI : Page 3

C_L	C_{D_T}	ΔC_{D_P}	S_T ft²	S_W	M.A.C	C at Nac.	D ft.	M M_L L	No. Engines	$\Delta C_{L_{MAX}}$	ΔC_{M_o}	$\Delta\left(\frac{dC_M}{dC_L}\right)$	i	α_{OL}	i_W	η_*	$\frac{\eta}{c}$	Cooling Flow	$\frac{dC_{m_{F2}}}{d\alpha_{(rad.)}}$	$\frac{dC_{m_{F_1}}}{d\alpha_{rad.}}$	GALCIT Report No.	Nacelle Notation	Remarks
0.3	.071	.0030	39.8	1422	11.55'	13.8	6.0	M_L	4	-.06	.033	.027	30°	-2°	5°	.86	.58	No	2.09	2.90		No_{11}	
.4	.049	.0016	35.8	1048	123.6"	12.1'	5.04	M_L	"	-.06	.013	.040	"	-1.2°	42°	.84	.522	No	2.38	5.57	285	N_I,	
.4	.065	.0021	38.8	1048	"	9.12'	5.04	M_L	"	0	.006	.036	"	"	"	"	.717	"	4.89	6.65		N_{O_1}	
.2	.058	.0015	26.8	"	123.5"	12.2'	4.13	M_L	"	-	.007	.030	"	-2°	5°	.83	.54	"			279	N_I	
"	.074	.0019	"	"	"	9.1'	"	M_L	"	-	.011	.024	"	"	"	"	.75	"				N_O	
"	.045	.0016	37.1	"	"	12.2'	4.86	M	"	-	.025	.045	"	"	"	"	.615	"				N_{I_3}	
"	.059	.0021	"	"	"	9.90'	4.86	M	"	-	.007	.029	"	"	"	"	.804	"				N_{O_3}	
"	.042	.0015	"	"	"	12.2'	4.86	M	"	-	.027	.025	"	"	"	"	.54	"				N_{I_1}	
"	.040	.0014	"	"	"	12.2'	4.86	M	"	-	.027	.019	"	"	"	"	.42	"				N_{I_2}	
.2	.114	.0061	78.48 4 NACELLES	1462	168.56"	—	5'	M	"	-0.10	.010	.048	20°	-5.2°	7.2°	.76	-	Yes			271	N	DC-4
.35	.109	.0089	38.0		100.23"	9.32	4.92'	L	2	-	-	-	30°	-3.7°	6.7°	.71	.317	Yes			263	N_4C_1	A-20
"	.104	.0085	"	"	"	"	"	"	"	-	.022	.026	"	"	"	"	"	Yes				$N_4C_1P_1$	
"	.086	.0070	"	"	"	"	"	"	"	-	-	-	"	"	"	"	"	No				N_4C_{1c}	
"	.088	.0072	"	"	"	"	"	"	"	-	.018	.026	"	"	"	"	"	No				$N_4C_{1c}P$	
"	.108	.0054	63.6	1267	9.00'	-	-	-	4	-	-	-	"	"	"	"		No			258	N_2N_O	LB-25
.45	.041	.0013	40.4	"	11.05'	12.9'	4.92	M	2	-	.007	.020	0	-2°	2°	.84	.644	No			257	N	CONSAIR B/M-7
"	.038	.0010	33.8	"	"	"	5.92	M	"	-	-	-	0°	"	"	"	.72	No				N_1	
"	.038	.0012	404	"	"	"	4.92	M	"	-	-	-		"	"	"	.644	"			257-A	N	
"	.026	.0007	33.8	"	"	"	5.92	"	"	-	-	-	"	"	"	"	.72	"				N_1	
"	.041	.0014	43.3	"	"	"	5.25	"	"	-	.012	.024	"	"	"	"	.568	"				N_2	
0"2	.118	.0075	88.28	602.1	116.39"	13.2'	4.93	L	2	-0.08	.000	.043	3°	-1°	4°	.72	.414	Yes			253	N_HC	NA 62
"	.095	.0060	"	"	"	"	"	"	"	-	-	-	"	"	"	"	.414	No				N_HC	
"	.120	.0076	"	"	"	"	"	"	"	-0.07	-	.051	"	"	"	"	"	Yes				NC	
"	.115	.0073	"	"	"	"	"	"	"	-0.08	-	.043	"	"	"	"	"	Yes				$N_BCX_{N_2}$	
"	.081	.0043	33.2	"	"	"	4.60	"	"	-.04	-	.059	"	"	"	"	.47	No				N_2C_2	

TABLE VI: Page 4

C_L	C_{D_P}	ΔC_{D_P}	S_P ft.²	S_W ft.²	M.A.C.	C at Nac.	D ft.	M_L	No. Engines	$\Delta C_{L_{MAX}}$	ΔC_{M_o}	$\Delta\left(\frac{dC_M}{dC_L}\right)$	i	α_{o_L}	i_W	η_{ac}	$\frac{n}{c}$	Cooling Flow	$\frac{dC_{m_{F_2}}}{d\alpha}$	$\frac{dC_{m_{F_1}}}{d\alpha}$	GALCIT Report No.	Nacelle Notation
0.2	.080	.0048	33.2	603.1	116.89"	13.2	4.6)	L	2	-.06	-	.059	3°	-1°	4°	.72	.47	No			253	N_2C_3
0.2	.086	.0055	38.8	"	"	"	4.97	"	"	-.05	-	.058	"	"	"	"	.37	-				$N_3C_4X_{N_4}$
.2	.123	.0071	35.1	609.35	"	"	4.72	"	"	-.02	.003	.047	"	"	"	.72	.47	Yes			253-A	N_aX_NC
.2	.108	.0062	"	"	"	"	"	"	"	.04	-	-	"	"	"	"	"	No				$N_{ac}.CA_F$
"	.134	.0077	"	"	"	"	"	"	"	-.03	-	-	"	"	"	"	"	Yes				N_SCA_F
"	.142	.0084	36.0	"	"	"	4.78	"	"	-	-	-	"	-1.1	4.1	"	.458	"			253-B	N_5C_5
.4	.053	.0025	49.8	1048	10.30'	11.9'	5.40'	M	"	-	.006	.028	0°	-2°	2°	.84	.53	No			251 CONSAIR MODEL 31	N
"	.040	.0019	"	"	"	"	"	"	"	-	"	"	"	"	"	"	"	"				N_1
"	.040	.0019	"	"	"	"	"	"	"	-	"	"	"	"	"	"	"	"				N_2
"	.042	.0020	"	"	"	"	"	"	"	-	"	"	"	"	"	"	"	"				N_3
0.3	.072	.0015	26.466	1267	132.6"	13.1'	1.63	"L	4	-	.004	.011	3°	-2.1°	5.1°	"	.39	"			249 CONSAIR LC-4	N_{IN}
"	.043	.0009	26.348	"	"	"	5.25	"	"	-	.005	.025	"	"	"	"	.52	"				N_{I_F}
"	.087	.0009	13.148	"	"	"	2.89	"	"	-	.007	.018	"	"	"	"	.67	"				N_{I_C}
"	.062	.0018	36.644	"	"	"	4.83	"L	"	-	.009	.031	"	"	"	"	.61	"				N_{I_R}
.3	.148	.0052	34.68	987	11.52'	"	4.70'	"	2	-	-	-	2°	-	-	-	-	-			244-DC-3	
.2	.059	.0015	26.8	1048	123.68"	12.2'	4.13	"L	4	-	.012	.025	3°	-2.0°	5°	.82	.54	"			243 B-24	N_I
"	.065	.0016	"	"	"	9.1'	4.13	"L	"	-	.009	.021	"	"	"	"	.76	"				No
.2	.072	.0052	78.7 4 NACELLES	1000	129'	12.2' AVG. FOR 4	4.82	"	"	-	.005	.030	"	-4.4°	7.4°	.76		"			242 Lockheed 44	VALUES FOR 4 NACELLES
.2	.110	.0080	"	"	"	—	"	"	"	-	.004	.036	"	"	"	"		Yes				
.2	.056	.0014	20.5	800	120'	12.5'	3.17	"	3	-	.003	.021	"	-4°	7°	.74		No			240 TRANSAIR	N_{10}
.2	.090	.0023	29.5	"	"	"	4.33	"H	3	-	.007	.040	"	"	"	"		"				N_{20}
.2	.072	.0036	27.	538.5	9.69'	11.2'	4.14	M	2	-	.007	.037	2.5°	-3.2°	5.7°	.79	.355	"			239	
"	.088	.0044	27	"	"	"	"	"	"	-	.007	.034	"	"	"	"	"	Yes				N_L
"	.084	.0040	25.7	"	"	"	3.4	"L	"	-	.007	.041	"	-3.2° COMPLETE MODEL	5.7°	"	.79	"				N_3'

TABLE VI : Page 5

C_L	C_{D_m}	ΔC_{D_p}	S_m ft²	S_w ft²	M.A.C.	C at Nac.	D ft.	M / M_L	No. Engines	$\Delta_{L_{MAX}}$	ΔC_{M_0}	$\Delta\left(\frac{dC_M}{dC_L}\right)$	i	α_{o_L}	i_w	η_m	$\frac{n}{c}$	Cooling Flow	$\frac{dC_{m_{F_2}}}{d}$	$dC_{m_{F_1}}$	GALCIT Report	Nacelle Notation
.2	.103	.067	8.5	749	114.1"	10.8'	4.78	L	2	-	.012	.047	2°	-3.9°	5.9°	.74	.512	Yes			238	N_1
.2	.158	.042	31.8	598.5	116.2"	10.85'	4.50	L	2	-	.025	.050	-	-3.8°	-	.72	.52	No			237	NX_N
.2	.31	.059	38.8	598.5	116.2"	11.1'	4.37	L	"	-	.050	.048	-	-4.0	-	"	.37	Yes			236 NA-40	N_3X_4
"	.36	.036	38.8	"	"	"	"	"	"	-	.035	.050	-	"	-	"	"	"				$N_1X_{N_1}$
"	.38	.057	"	"	"	"	"	"	"	-	-	"	-	"	-	"	"	"				$N_2X_{N_2}$
																					234	SEPARATE NACELLE RUNS NOT MADE
.2	.08	.016	26.8	1048	138.5"	11.2'	4.13	M	4	-	.012	.062	3°	-1.8°	4.8°	.85	.46	No			234-A CONSAIR MODEL 32	N_I
"	.102	.026	"	"	"	"	"	"	"	-	.004	.035	"	"	"	"	"	"				N_{I_2}
"	.083	.0021	"	"	"	9.1'	"	"	"	-	-	-	"	"	"	"	.76	"				N_{C_2}
"	.140	.0051	43.65	1201.5	160.80"	14.26'	5.22	M	2	-	.000	.039	0°	-1°	1°	.74	.40	Yes			227 Lockheed 27	N_3
	.130	.0049	40.0	1200.8	158.80'	14.4'	5.04	M	2	-	.000	.040	3°	-1.8°	4.8°	.76	.30	"			225 Lockheed 27	N_1
.3	.074	.0017	24.2	1048	10.27'	9.75	1.44	M_L	3	-	.015	.010	0°	-1.3°	1.9°	.85	.21	No			224 CONSAIR	N
.5	.070	.0028	41.8	"	"	11.9'	4.84	M	2	-	.0	.022	"	-2°	2°	.84	.34	No			222 CONSAIR 32	N_1
.5	.065	.0031	49.8	"	"	"	5.54	M	2	-	.003	.030	"	"	"	.84	.42	No				N_2
.5	.111	.0032	51.2	1780	193.5"	17.2' AVE. FOR 4	4.04	M	4	-	.000	.020	3°	-1.6°	4.6°	.73	.28 AVE.	No			221 CONSAIR XPB2Y-1	N_C } VALUES FOR 4
.5	.066	.0032	86.0	"	"	-	5.415	M	4		-	-	"	"	"	"	-	No				N_2 } NACELLES
.5	.084	.0029	61.2	"	"		4.13	M	4		.010	.028	"	"	"	"	.376	No			221-A	N_5
.5	.052	.0022	42.2	1000	10.58'	13.2'	4.88	M	2		-	-	2°	-1.9°	3.9°	.80	-	No			218 CONSAIR MODEL X	N
.5	.080	.0025	80.0	"	"	12.2'	5.32	M	2	-	.005	.040	0°	"	1.9°	"	-	No				N_2
.4	.113	.0029	46.9	1253	10.69	12.37'	5.45	M_L	2	-	.012	.042	2.5°	-1.2°	3.7°	.73	.384	Yes			208 CW-20	N
.4	.095	.0033	46.9	"	"	"	"	"	"	-	.015	.035	2.5°	"	3.7°	"	"	No			203 "	N_C
.5	.147	.0019	43.8	8395	19.005'	13.46'	4.69	M	4	-	.008	.010	5°	-.8°	5.5°	.84	.474	Yes			199	N_{OUT}
"	.100	.0016	54.0	"	"	23.3'	5.40	M	4	-	-	-	"	"	"	"	.396	Yes			199	N_{IN}
.25	.144	.0073	38.5	471	110."	10.6'	3.85	M_L	2	-	.006	.028	0°	-3.6°	5.6°	.79	.584	Yes			193 LOCKHEED S-16	$N_2C_2I_2(S_E)$
.25	.139	.0069	"	"	"	"	"	M_L	2	-	-	-	-	-	-	-	-	yes				$N_2C_1I_2(S_E)$

TABLE VI : Page 6

C_L	C_{D_m}	ΔC_{D_p}	S_m ft.²	S_w ft.²	M.A.C.	C at Nac.	D	M_L	No. Engines	$\Delta C_{L_{MAX}}$	ΔC_{M_0}	$4\left(\frac{dC_m}{dC_L}\right)$	i	α_{0_L}	i_w	η_*	$\frac{\eta}{c}$	Cooling Flow	NACELLE NOTATION	GALCIT REP. NO.	REMARKS
.4	.095	.0032	34.8					M	2									Yes	N_1 L_r	191	DC-3R
"	.093	.0051	56.7					M_L	2									"	N_2		
"	.086	.0047	"					M_L	2									"	N_3		
.5	.126	.0031	71.	2880				M	4									N_o	N_1	190	1 CONSAIR XPB3Y-1
"	.077	.0019	"	2866				M	4									No	N_2		
"	.086	.0022	"	2785				M	4									Yes	N_3		
.2	.117	.0070	33.1	551	115.8"	4.6'	11.36'	M_L	2		.012	.058	2°	-0.8°	2.8°	.75	.44	Yes		187	LOCKHEED 14
.3	.169	.0032	26.48	1402	13.78'	15'	4.1'	M	2		.002	.009	-	-1.8°	-	.75	.27	Yes	N (ORIGINAL)	178	PBY-1
.3	.154	.0029	"	"	"	"	"	M	2		-	-	-	-	-	.75	"	"	N(MOVED)		
.3	.110	.0066	33.1	551	115.8"	4.6'	11.2'	M_L	2		.030	.022	2°	-1.8°	3.8°	.81	.46	"	$N_2C_3I_{4c}$	177	Lockheed S-10
.2	.076	.0024	68.0	2155	17.7'	19.8' AVE.	4.65'	M	4		.005	.026	-	-5°	-	.77	.35	-		175	DC-4 VALUES FOR 4 NACELLES
	.112	.0070	25.1					M	2									YES		174	Northrup 7-A
	.082	.0039	11.67					-	2									"		173	Lockheed S-10
	.128	.0041	38.3					L	2									"		171	N.A. -21 Bomber
	.115	.0032	9.8					M_L	2									"	MENASCO	161	Lockheed C-12
	.067	.0045	23.6					M	2									"	C_2N_{1B}	159 157	C
	.096	.0027	54.8					M	4									"		152	C.W. P. 212
	.085	.0030	68.4					M	4									"	CYCLONE		
	.147	.0062	60.0					M_L	4									"	WASP	145	Boeing 299, 300
	.168	.0078	66.0					M_L	4									"	HORNET		
	.075	.0040	15.0						2											138	Lockheed, ALCOR
	.077	.0027	33.0					M	2									YES		132	DOUGLAS DC-1
	.071	.0018	33.0					M	2									"	SINGLE ROW	159	Douglas DF
	.150	.0030	26.0					M	2									"	DOUBLE ROW	159	Douglas "
	.292	.0064	28.4					-	2									"	RAISED	157 129	DOUGLAS
	.128	.0028	"					-	2									"	L.E.	157 129	Douglas
	.224	.0067	33.0						2									"	RAISED	126	" YOA-5